bone regeneration in combination with a modified poly-DL-lactic-co-glycolic acid (PLGA)-collagen sponge. J. Cell Physiol. 194:45–53.
27. **Okamoto, T., T. Aoyama, T. Nakayama, T. Nakamata, T. Hosaka, K. Nishijo, T. Nakamura, T. Kiyono, and J. Toguchida.** 2002. Clonal heterogeneity in differentiation potential of immortalized human mesenchymal stem cells. Biochem. Biophys. Res. Commun. 295:354–361.
28. **Olsen, B. R., A. M. Reginato, and W. Wang.** 2000. Bone development. Annu. Rev. Cell Dev. Biol. 16:191–220.
29. **Park, I. K., D. Qian, M. Kiel, M. W. Becker, M. Pihalja, I. L. Weissman, S. J. Morrison, and M. F. Clarke.** 2003. *bmi-1* is required for maintenance of adult self-renewing haematopoietic stem cells. Nature 423:302–305.
30. **Sano, M., A. Umezawa, H. Abe, A. Akatsuka, S. Nonaka, H. Shimizu, M. Fukuma, and J. Hata.** 2001. EAT/mcl-1 expression in the human embryonal carcinoma cells undergoing differentiation or apoptosis. Exp. Cell Res. 266: 114–125.
31. **Santa-Olalla, J., and L. Covarrubias.** 1995. Epidermal growth factor (EGF), transforming growth factor-alpha (TGF-alpha), and basic fibroblast growth factor (bFGF) differentially influence neural precursor cells of mouse embryonic mesencephalon. J. Neurosci. Res. 42:172–183.
32. **Satoh, J., and Y. Kuroda.** 2002. The constitutive and inducible expression of Nurr1, a key regulator of dopaminergic neuronal differentiation, in human neural and non-neural cell lines. Neuropathology 22:219–232.
33. **Scheffner, M., K. Munger, J. M. Huibregtse, and P. M. Howley.** 1992. Targeted degradation of the retinoblastoma protein by human papillomavirus E7-E6 fusion proteins. EMBO J. 11:2425–2431.
34. **Schrock, E., T. Veldman, H. Padilla-Nash, Y. Ning, J. Spurbeck, S. Jalal, L. G. Shaffer, P. Papenhausen, C. Kozma, M. C. Phelan, E. Kjeldsen, S. A. Schonberg, P. O'Brien, L. Biesecker, S. du Manoir, and T. Ried.** 1997. Spectral karyotyping refines cytogenetic diagnostics of constitutional chromosomal abnormalities. Hum. Genet. 101:255–262.
35. **Sekiguchi, T., and T. Hunter.** 1998. Induction of growth arrest and cell death by overexpression of the cyclin-Cdk inhibitor p21 in hamster BHK21 cells. Oncogene 16:369–380.
36. **Terai, M., T. Uyama, T. Sugiki, X. K. Li, A. Umezawa, and T. Kiyono.** 2005. Immortalization of human fetal cells: the life span of umbilical cord blood-derived cells can be prolonged without manipulating p16INK4a/RB braking pathway. Mol. Biol. Cell 16:1491–1499.
37. **van Lohuizen, M., S. Verbeek, B. Scheijen, E. Wientjens, H. van der Gulden, and A. Berns.** 1991. Identification of cooperating oncogenes in E mu-myc transgenic mice by provirus tagging. Cell 65:737–752.
38. **Wright, W. E., and J. W. Shay.** 1992. The two-stage mechanism controlling cellular senescence and immortalization. Exp. Gerontol. 27:383–389.
39. **Zetterstrom, R. H., L. Solomin, L. Jansson, B. J. Hoffer, L. Olson, and T. Perlmann.** 1997. Dopamine neuron agenesis in Nurr1-deficient mice. Science 276:248–250.

Available online at www.sciencedirect.com
SCIENCE DIRECT®
ELSEVIER
Biochemical and Biophysical Research Communications 332 (2005) 1004–1011
BBRC
www.elsevier.com/locate/ybbrc

Laminin binding protein, 34/67 laminin receptor, carries stage-specific embryonic antigen-4 epitope defined by monoclonal antibody Raft.2

Yohko U. Katagiri [a,b,*], Nobutaka Kiyokawa [a], Kyoko Nakamura [c], Hisami Takenouchi [a], Tomoko Taguchi [a], Hajime Okita [a], Akihiro Umezawa [d], Junichiro Fujimoto [a]

[a] *Department of Developmental Biology, National Research Institute for Child Health and Development, Setagaya-ku, Tokyo 157-8535, Japan*
[b] *Japan Science and Technology Corporation, CREST, Japan*
[c] *Supra-Biomolecular System Research Group, RIKEN Frontier System Research, Wako-shi, Saitama 351-0198, Japan*
[d] *Department of Reproductive Biology, National Research Institute for Child Health and Development, Setagaya-ku, Tokyo 157-8535, Japan*

Received 24 April 2005
Available online 23 May 2005

Abstract

We previously produced monoclonal antibodies against the detergent-insoluble microdomain, i.e., the raft microdomain, of the human renal cancer cell line ACHN. Raft.2, one of these monoclonal antibodies, recognizes sialosyl globopentaosylceramide, which has the stage-specific embryonic antigen (SSEA)-4 epitope. Although the mouse embryonal carcinoma (EC) cell line F9 does not express SSEA-4, some F9 cells stained with Raft.2. Western analysis and matrix-assisted laser desorption ionization-time of flight mass spectrometry identified the Raft.2 binding molecule as laminin binding protein (LBP), i.e., 34/67 laminin receptor. Weak acid treatment or digestion with *Clostridium perfringens* sialidase reduced Raft.2 binding to LBP on nitrocellulose sheets and [^{14}C]galactose was incorporated into LBP, indicating LBP to have a sialylated carbohydrate moiety. Subcellular localization analysis by sucrose density-gradient centrifugation and examination by confocal microscopy revealed LBP to be localized on the outer surface of the plasma membrane. An SSEA-4-positive human EC cell line, NCR-G3 cells, also expressed Raft.2-binding LBP.

Keywords: SSEA-4; SialylGb5; Embryonal carcinoma; Laminin binding protein; Laminin receptor; Raft.2; MALDI-TOF MS

EC derived from testicular teratocarcinomas are a subset of germ cell tumors that may contain many embryonic and extra-embryonic tissues, and they represent malignant replicas of normal embryonic cells at specific stages of development. Immunochemical markers, such as SSEA-1, -3, and -4, TRA-1-60, and TRA-1-81, have been utilized to characterize and define the developmental stages of EC lines. For example, early cleavage-stage mouse embryos [1] and the primitive and visceral yolk sac endodermal cells of post-implantation mouse embryos [2] express SSEA-3 and SSEA-4. These carbohydrate antigens are also found on human, but not on murine, EC cells [3]. By contrast, murine EC cells express SSEA-1, while human EC cells do not. Exposure to retinoic acid can prompt EC cells to develop to advanced stages, accompanied by changes in SSEA expressions. Many monoclonal antibodies defining SSEAs were generated in early studies of mammalian development. SSEA-1 is an antigenic epitope defined as a Lewis x (Le^x) carbohydrate structure and is found in both glycosphingolipids and glycoproteins [1,4]. SSEA-3 and -4 defined by MC631 and MC813-70, respectively,

* Corresponding author. Fax: +81 3 3487 9669.
E-mail address: kata@nch.go.jp (Y.U. Katagiri).

0006-291X/$ - see front matter © 2005 Elsevier Inc. All rights reserved.
doi:10.1016/j.bbrc.2005.05.052

are located in carbohydrate moieties of globoseries glycosphingolipids [5].

We previously established a monoclonal antibody (Mab) termed Raft.2 by subcutaneously injecting the raft microdomain of a human renal cancer cell line, ACHN, into Balb/c mice and showed that Raft.2 recognizes the carbohydrate structure of sialosyl globopentaosylceramide (sialylGb5), namely GL7, the epitope of SSEA-4 [6]. SSEAs are still among the best markers for characterizing embryonic stem (ES) cells or EC cells and Raft.2 is a potentially useful tool for this purpose.

Although mouse EC F9 cells are known to be SSEA-4 negative, some of these cells stained with Raft.2. In this study, we demonstrated that Raft.2 binds to LBP and that Raft.2-positive LBP is present not only in F9 cells, but also in human EC NCR-G3 cells. We also show LBP to be localized on surface membranes and discuss the significance of LBP carrying SSEA-4. This is the first report, to our knowledge, focusing the SSEA-4 carried by LBP.

Materials and methods

Cell culture and antibodies. The mouse EC cell line F9 and the human renal cancer cell line ACHN were purchased from the American Type Culture Collection. F9 cells were cultured in Dulbecco's modified Eagle's medium (DMEM) (Sigma Chem., St. Louis, MO) supplemented with 10% fetal bovine serum (Sigma). ACHN was cultured in Eagle's minimum essential medium (MEM) (Sigma) supplemented with 10% fetal bovine serum and the non-essential amino acid solution (Sigma). The human EC cell line, NCR-G3 [7], was cultured in a 1:1 mixture of DMEM and Ham's F12 medium (Gibco, Grand Island, NY) supplemented with 10% fetal bovine serum, insulin–transferrin–sodium selenite media (Sigma), and the non-essential amino acid solution. MC-631, Mab for SSEA-3 and MC-813-70, Mab for SSEA-4, to detect Gb5 and sialylGb5, respectively, were purchased from Chemicon International (Temecula, CA). 13C4, Mab for Shiga toxin 1-B subunit (Stx1B), and T-20, a rabbit anti-mouse GTP binding protein β subunit (Gβ) polyclonal antibody, were purchased from the American Type Culture Collection and Santa Cruz Biotechnology (Santa Cruz, CA), respectively.

Glycolipid analysis. The packed cell pellet (0.5 ml) was extracted with 2 ml chloroform/methanol (C/M) (2:1, v/v) and then with 2 ml of chloroform/isopropanol/water (7:11:2, v/v). Total extracts were combined and evaporated to dryness and then treated with 0.2 N KOH in methanol at 37 °C for 2 h to saponify the phospholipids. After neutralization, methyl esters of fatty acids were removed by mixing with hexane. The extracts were then concentrated to 1/10 volume and dialyzed against water. The retentate was freeze-dried and dissolved in C/M (2:1).

Thin layer chromatography (TLC) immunostaining was performed according to a previously described method [8]. Briefly, C/M extracts were separated on plates precoated with Silica gel 60 (HPTLC aluminium sheets, Merck, Darmstadt Germany) using a solvent system consisting of C/M/water containing 0.1% $CaCl_2$ (5:4:1, v/v/v). After drying, the plates were dipped in 0.1% polyisobutylmethacrylate (Aldrich Chem., Milwaukee, WI, USA) in cyclohexane for 1 min and blocked with 1% bovine serum albumin (BSA) in phosphate-buffered saline (PBS). The plates were probed with Shiga toxin 1-B subunit (Stx1B) (1 μg/ml in 1% BSA) [9], then Mab 13C4 culture supernatant to detect globotriaosylceramide (Gb3), and with Mab Raft.2 culture supernatant to detect sialylGb5. After three washes with PBS for 5 min each, horseradish peroxidase-conjugated rabbit anti-mouse immunoglobulins (DAKO, A/S, Denmark) at a 1:2000 dilution ratio were used as the second antibody. The antibodies that bound to the plates were visualized with enhanced chemiluminescence reagent SuperSignal (Pierce, Rockford, IL, USA) and detected by LAS-1000 (Fuji Film, Tokyo, Japan).

Flowcytometry. Cells were harvested and incubated with a 1st antibody for 1 h on ice, followed by treatment with fluorescein isothiocyanate-conjugated goat anti-mouse immunoglobulins (Jackson Laboratory, West Grove, PA) at a 1:50 dilution ratio and analyzed by flowcytometry (EPICS-XL, Beckman–Coulter).

Western analysis. Cells were homogenized in hypotonic buffer (25 mM NaCl, 0.5 mM $CaCl_2$, 18 mM Tris–HCl buffer, pH 8.0) and cell debris was removed by centrifugation at 200*g* for 5 min at 4 °C. Precipitates were homogenized in the same manner two more times. The combined supernatants were centrifuged at 40K rpm for 30 min at 4 °C in a Beckman 80Ti rotor to obtain crude membrane fractions. The membrane proteins released with 1% Triton X-100 in 25 mM Tris–HCl buffer, pH 7.5, containing 0.15 M NaCl and the cocktail of protease inhibitors, were subjected to 1-dimensional (1-D) or 2-D Western analysis as previously described [10]. In order to remove the sialic acids from the glycoproteins, after 1-D Western blotting, the membrane strips were treated with 25 mM H_2SO_4 at 80 °C for 1 h.

Matrix-assisted laser desorption ionization-time of flight mass spectrometry (MALDI-TOF MS) analysis. The membrane proteins were separated by 2-D polyacrylamide gel electrophoresis (PAGE) and stained with Coomassie brilliant blue (CBB) R-250 (Bio-Rad Lab., Richmond, CA). The CBB-stained protein that corresponded to the position of the Raft.2-reacting spot was excised and digested with trypsin, and the trypsinized peptides were analyzed with an oMALDI-Qq-TOF MS/MS QSTAR Pulser *i* (Applied Biosystems). The mass spectra search was conducted using an NCBI non-reductant database with the MASCOT search algorithm.

Metabolic labeling of F9 cells with [^{14}C]galactose. Subconfluent cells (approx. 1.4×10^6 cells) were cultured in 4 ml of the incubation medium containing 10 μCi D-[1-^{14}C]galactose (57 mCi/mmol, 200 μCi/ml, Amersham Biosciences UK) for 24 h in a 60 mm culture plate. [^{14}C]Galactose-labeled membrane protein was prepared as above and mixed with 50 μg of non-labeled F9 membrane proteins. The F9 membrane protein mixture thus obtained was separated by 2-D PAGE and stained with CBB. Autoradiograms were obtained with BAS 2000.

Sialidase treatment. Proteins on 2-D nitrocellulose sheets were stained with Ponceau 3R Stain Solution (Wako Pure Chem., Osaka, Japan) and the rectangle containing the proteins of interest was excised. The blots were incubated in 50 mM sodium acetate buffer, pH 4.5, containing 0.1% BSA, with or without 100 mU of neuraminidase from *Clostridium perfringens* (Roche Diagnosis GmbH, Mannheim, Germany) at 37 °C overnight.

Subcellular fractionation. Crude membrane fractions obtained as described above were thoroughly suspended in the hypotonic buffer containing 30% sucrose and overlaid on a discontinuous sucrose density gradient of 40%/45%/50%/60% in a 12-ml ultracentrifugation tube, and the suspension was then overlaid with a 20% sucrose layer. The gradient was centrifuged at 25K rpm for 1 h in a Beckman SW40Ti rotor, and after recovery and dilution with PBS, each of the interface layers was sedimented at 40K rpm for 0.5 h in a Beckman 80Ti rotor. Proteins were released from each precipitate with 1% Triton X-100 lysis buffer and subjected to 2-D PAGE.

Staining for fluorescence microscopic observation. EC cells were harvested from cell culture plates and incubated with Raft.2. They were then stained with Alexa Fluor 488-conjugated goat anti-mouse IgM, μ-chain (Molecular probes, Eugene, OR) for 1 h and mounted in Perma Fluor Aqueous Mounting Medium (Thermo Shandon, Pittsburgh, PA) on a slide glass. The slides were observed with an Olympus LSM-GB200 confocal microscope.

Results

The sialylGb5 expressions on murine and human EC cells were examined by TLC immunostaining and flowcytometry with two Mabs against SSEA-4, Raft.2, and MC-813-70. ACHN cells, which express globoseries glycolipids, such as Gb3 and sialylGb5, were also examined and compared, as a control. All of these cell lines synthesized Gb3 (Fig. 1A, left panel). SialylGb5 was synthesized by ACHN and NCR-G3, but not F9, cells (Fig. 1A, right panel). ACHN and NCR-G3 cells were confirmed to express both sialylGb5 and Gb5 on their surface by flowcytometry (Fig. 1B, upper and lower row). Flowcytometric analysis further confirmed SSEA-4 expression on small populations (8.42%+) of F9 cells using Raft.2 and the faint expression using MC-813-70 (Fig. 1B, middle row). The staining profile of MC-631 was similar to that of Raft.2 (6.7%+). Taking these observations together, although F9 cells do not synthesize sialylGb5, they clearly express the SSEA-4 epitope on their surfaces.

We performed Western analysis to ascertain whether the SSEA-4-carried molecules are glycoproteins. Cytoplasmic proteins and 1% Triton membrane lysates of F9 cells were subjected to 1-D and 2-D Western analysis. Mab Raft.2 definitely bound to a membrane protein with an apparent molecular weight (mw) of 44K (Fig. 2A), but did not bind to cytoplasmic proteins (data not shown). Since Raft.2 cannot bind to Gb5, sialic acid residue is prerequisite for Raft.2 binding to the SSEA-4 epitope. Weak acid treatment of the blot markedly diminished Raft.2 binding to the 44K protein, while only minimally decreasing T-20 binding to its antigen, Gβ. These findings indicate that the carbohydrate chain of the protein is sialylated. 2-D Western analysis yielded

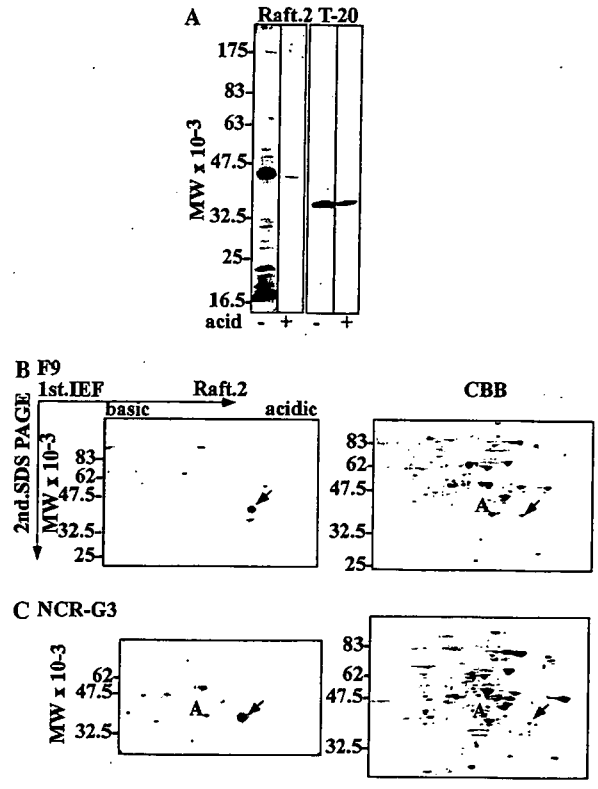

Fig. 2. Western analysis of the Raft.2 binding protein. (A) Membrane proteins of F9 cells were separated to four lanes by 1-D SDS–PAGE and transferred to a nitrocellulose sheet. Two of the strips were treated with weak acid (+), the other two were not (−). Two (− and +) were probed with Raft.2 (left), the other two with T-20 (right). (B) The membrane proteins separated by 2-D PAGE were transferred to a nitrocellulose sheet and probed with Raft.2 (left panel) or the membrane proteins in a 2-D gel were stained with CBB (right panel). The arrow points to the spot bound by Raft.2 and "A" indicates actin. (C) Membrane proteins of NCR-G3 cells were analyzed as in (B).

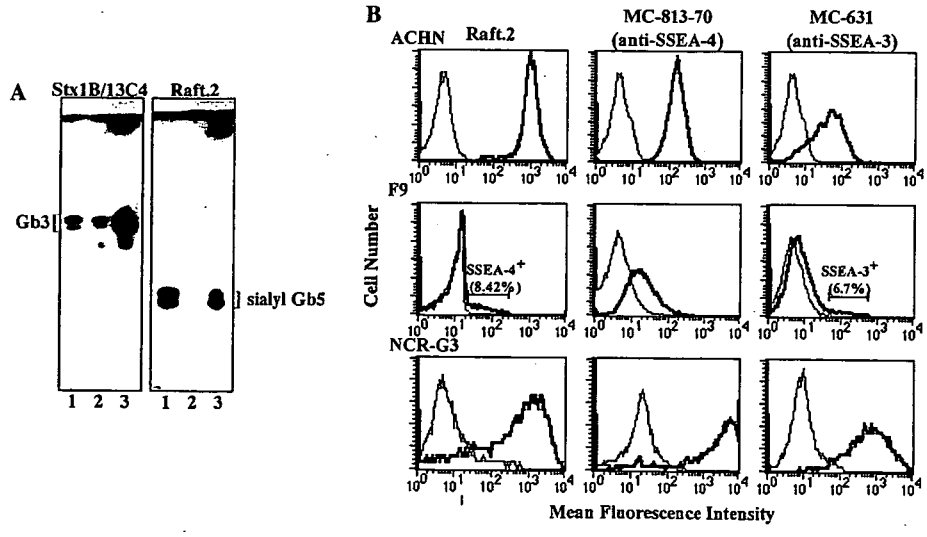

Fig. 1. Expression of SSEA-4 by the murine and human EC cell lines, F9 cells, and NCR-G3. (A) Total lipids from ACHN cells (lane 1), F9 cells (lane 2), and NCR-G3 cells (lane 3) were separated by TLC and immunostained with Stx1B/13C4 (left) and Raft.2 (right). (B) Cells were stained with Raft.2 (left row), MC-813-70 (middle row), or MC-631 (right row) and with a FITC-conjugate secondary antibody and analyzed by flowcytometry.

a single spot at an isoelectric point (p*I*) of 5.0 (Fig. 2B, left panel), slightly more acidic than actin (Fig. 2B, right panel). NCR-G3 cells expressed exactly the same Raft.2-positive proteins as F9 cells (Fig. 2C). The other two anti-SSEA Mabs, MC-813-70 and MC-631, bound none of the SDS-denatured proteins on a nitrocellulose sheet (data not shown).

In order to identify the spot bound by Mab Raft.2, we carried out MALDI-TOF MS/MS analysis of this spot in a 2-D gel (Fig. 2B). Eleven possible peptide signals with masses (*m/z*) of 912.6, 1200, 1203.6, 1291.7, 1419.8, 1615, 1698, 1740.9, 2082.1, 2172.2, and 2298.2, respectively, were detected (Fig. 3, underlined) and matched to the fragments of 40S ribosomal protein SA, known as 34/67 laminin receptor or LBP. The MS/MS spectra of five peptides (*) were obtained and the fragments were matched to the sequence from Lys_{42} to Arg_{128} of LBP (Table 1).

In order to confirm that LBP has a sialylated carbohydrate chain, we examined whether [^{14}C]galactose is incorporated into LBP. Membrane proteins prepared from F9 cells, which were metabolically labeled with [^{14}C]galactose, were separated by 2-D PAGE and subjected to autoradiography. The LBP spot was detected on the autoradiogram obtained by BAS 2000 (Fig. 4A). Next, we examined the effect of sialidase digestion on Raft.2 binding. Two nitrocellulose sheets, on which membrane proteins of NCR-G3 cells had been separated by 2-D PAGE followed by transfer, were stained with Ponceau 3R Stain (Fig. 4B). Small rectangles containing LBP were excised from the nitrocellulose sheets. The excised blot was incubated in 50 mM sodium acetate buffer, pH 4.5, with or without *C. perfringens* sialidase to release terminal sialic acids from glycoconjugates. This treatment reduced the Raft.2 binding to LBP (Fig. 4C), confirming that LBP contains sialic acid.

Table 1
Mass fragments fitted for murine LBP by Mascot search

m/z	Start	End	Peptide sequence
912.6*	121	128	LLVVTDPR
1200	54	63	TWEKLLLAAR
1203.6*	90	102	FAAATGATPIAGR
1291.7	43	53	SDGIYIINLKR
1419.8	42	53	KSDGIYIINLKR
1615*	86	102	AVLKFAAATGATPIAGR
1698	103	117	FTPGTFTNQIQAAFR
1740.9*	64	80	AIVAIENPADVSVISSR
2082.1*	103	120	FTPGTFTNQIQAAFREPR
2172.2	81	102	NTGORAVLKFAAATGATPIAGR

The five fragments (*) were subjected to MS/MS analysis.

Next, we fractionated the organelles of F9 cells by sucrose density gradient centrifugation to identify the

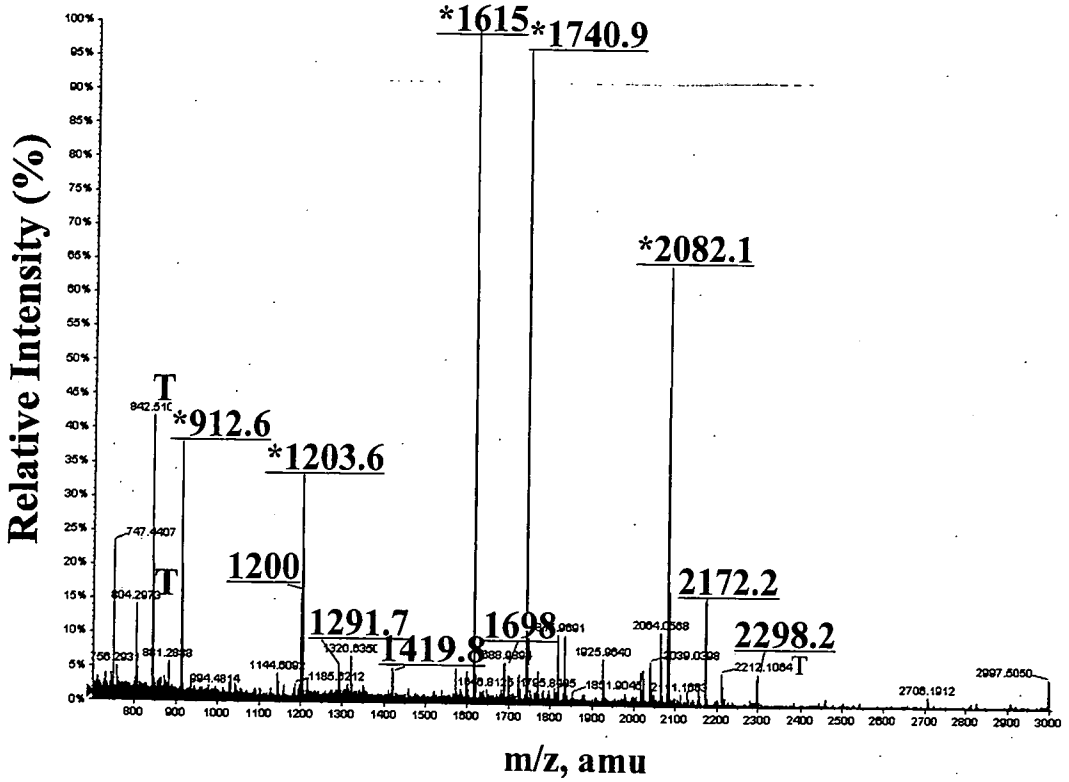

Fig. 3. MALDI-TOF MS spectra of the mw 44K molecule recognized by Raft.2. The Raft.2-binding molecule indicated by the arrow in Fig. 2C was in-gel digested with trypsin and subjected to oMALDI-Qq-TOF MS/MS QSTAR Pulser *i* spectrometry. The masses of the underlined peaks matched those of LBP. The peaks marked "T" were derived from trypsin.

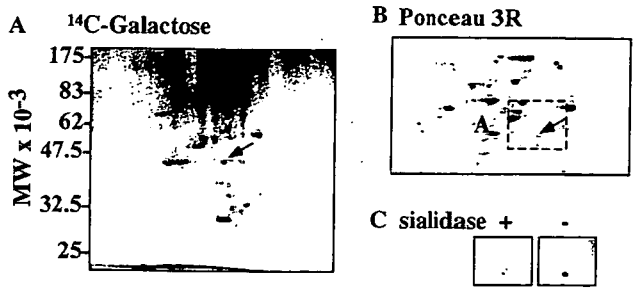

Fig. 4. Detection of galactose and sialic acid residues in LBP. (A) Autoradiogram of membrane proteins prepared from [^{14}C]galactose-labeled F9 cells and separated by 2-D PAGE. (B) The membrane proteins separated by 2-D PAGE were transferred to a nitrocellulose sheet and stained with Ponceau 3R. "A" indicates actin and the arrows point to LBP. (C) The blot containing LBP was incubated with (+) and without (−) sialidase and probed with Raft.2.

organelles in which LBP was localized. Triton X-100 lysates of each layer were 2-D separated and stained with CBB (Fig. 5). Since Src kinase Yes was found only in layer 1 (data not shown), the plasma membrane appears to be recovered from layer 1. Nuclear fragments were precipitated to the bottom. LBP was found only in layer 1, indicating that LBP is localized in plasma membranes.

fsConfocal microscopic observation confirmed Raft.2 binding on the cell surface. Cell suspensions of F9 and NCR-G3 were stained with Raft.2 and observed with a confocal microscope. Since Raft.1 recognizes Gβ located within cells [10], no F9 cells were stained with Raft.1 (Fig. 6A). As shown in Fig. 6B, some cells showed uneven, dot-like staining with Raft.2, while others did not. This indicates that some, not all, F9 cells express Raft.2 binding molecules on their cell surfaces. NCR-G3 cells were evenly stained with Raft.2 (Fig. 6C).

Discussion

We previously established Mab Raft.2, which specifically binds to sialylGb5 on TLC and cell surfaces. SialylGb5 carries the SSEA-4 epitope, which is naturally found in glycolipids. Interestingly, although mouse EC cell line F9 cells do not express sialylGb5, they are stained with Raft.2. Western analysis and the subsequent mass spectrometric analysis revealed the Raft.2 binding molecule to be LBP. The human EC cell line NCR-G3, which synthesizes sialylGb5, was also found to express Raft.2-binding LBP. Weak acid treatment or sialidase digestion reduced Raft.2 binding to LBP and [^{14}C]galactose was incorporated into LBP. These results confirm that LBP carries the SSEA-4 epitope. The precise carbohydrate structure of LBP must be obtained to provide further confirmation. Mass spectrometric analysis of the sugar moiety of LBP is currently underway, employing microLC-ESI MS/MS.

Raft.2 is different from another anti-SSEA-4 Mab, MC-813-70 in reactivity with SSEA-4 epitope. Raft.2 did not react with GM1b purified from mouse spleen [11] (data not shown), but MP-813-70 does [5]. These two Mabs appear to be different from each other in reactivity with glycoproteins.

Many developmentally regulated antigens, including SSEAs, ABH, Forssman, globoside, and Ii, are carbohydrates in nature [12]. Such antigenic determinants are carried by lipids and/or by protein molecules. It was previously reported that SSEA-1, i.e., Lewis x antigen (Le^x), is carried by both proteins [13] and lipids [4] and that SSEA-3 is carried by both membrane glycolipids and glycoproteins [1]. By contrast, it is generally accepted that the SSEA-4 is carried only by globoseries glycosphingolipids [5]. Herein, however, we present

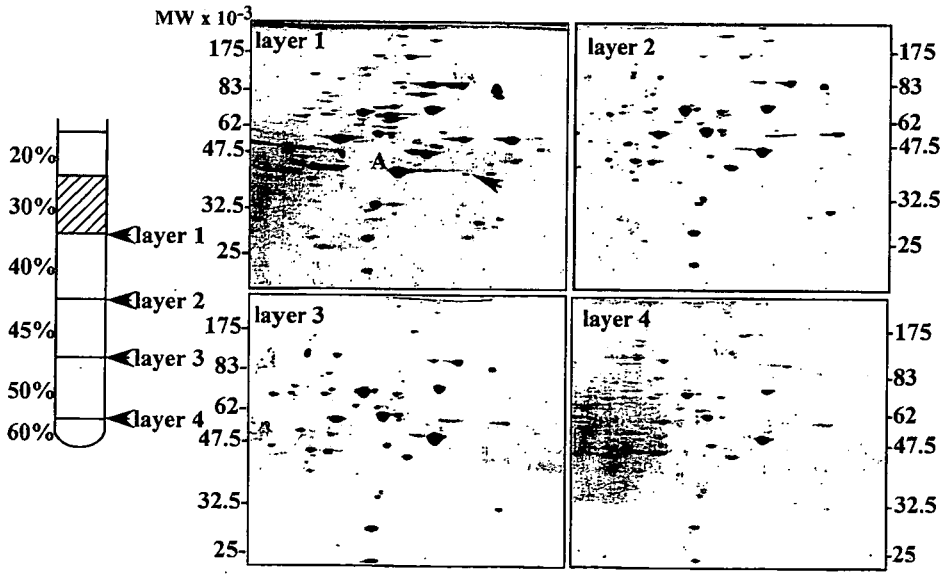

Fig. 5. Subcellular localization of LBP. The membrane proteins recovered from layers 1, 2, 3, and 4 after sucrose density-gradient centrifugation were analyzed by 2-D PAGE. The 2-D gels were stained with CBB. The arrow in the layer 1 gel points to LBP.

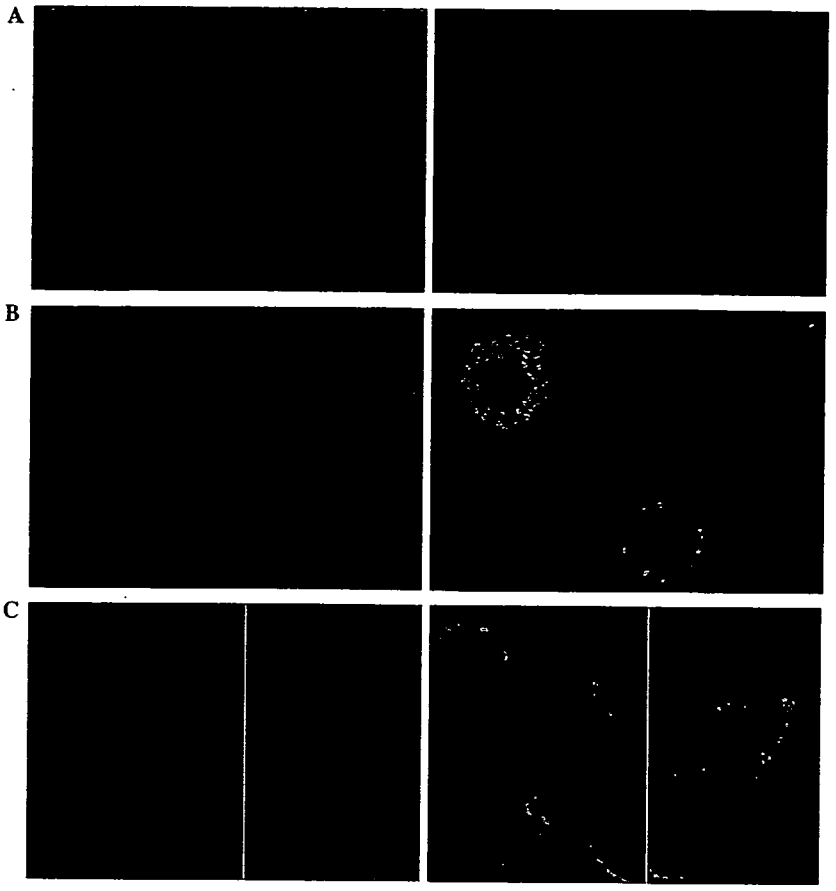

Fig. 6. Immunostaining of mouse and human EC cells with SSEA-4. Phase-contrast micrograph (left) and confocal micrograph (right). (A) Isotype-matched negative control Mab (Raft.1)/mouse EC F9—there is no staining. (B) Raft.2/F9—dot-like surface-staining. (C) Raft.2/human EC NCR-G3—even surface-staining.

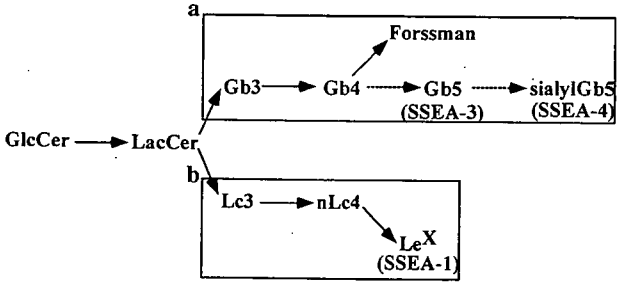

GlcCer:	Glcβ1→Cer
LacCer:	Galβ1,4Glcβ1→Cer
Gb3:	Galα1,4Galβ1,4Glcβ1→Cer
Gb4:	GalNAcβ1,3Galα1,4Galβ1,4Glcβ1→Cer
Forssman:	GalNAcα1,3GalNAcβ1,3Galα1,4Galβ1,4Glcβ1→Cer
Gb5:	Galβ1,3GalNAcβ1,3Galα1,4Galβ1,4Glcβ1→Cer
sialylGb5:	NeuAcα2,3Galβ1,3GalNAcβ1,3Galα1,4Galβ1,4Glcβ1→Cer
Lc3:	GlcNAcβ1,3Galβ1,4Glcβ1→Cer
nLc4:	Galβ1,4GlcNAcβ1,3Galβ1,4Glcβ1→Cer
Le^X:	Galβ1,4(Fucα1,3)GlcNAcβ1,3Galβ1,4Glcβ1→Cer

Fig. 7. Scheme summarizing the major glycosylation pathways in mouse EC F9 cells. The globoseries glycolipid synthesis pathway (a) and the neolactoseries glycolipid synthesis pathway (b) lead to the synthesis of SSEA-3 and -4 and SSEA-1 active glycolipids, respectively. The cells exhibit a distinct pattern of globo- and neolacto-series oligosaccharide chain elongation (solid arrows). Retinoic acid treatment converts the synthesis of Forssman to SSEA-3 and -4 (dotted arrows).

evidence that the SSEA-4 epitope is also carried by a protein, 34/67 laminin receptor, also called LBP.

In culture, the differentiation of murine EC or ES cells into endoderm-like cells is typically characterized by the loss of SSEA-1 expression and the appearance of SSEA-3 and SSEA-4 [14], and may be accompanied by up-regulation of laminin synthesis [15]. Laminins are a family of extracellular matrix proteins that constitute the major non-collagenous glycoproteins found in the basement membrane and are involved in multiple important biological activities, such as assembly of the basement membrane, cell attachment, migration, neurite outgrowth, and angiogenesis [16,17]. In addition, laminins have well demonstrated roles in diverse developmental processes, from the pre-implantation period onwards [18]. Laminin receptors are divided into two major groups: integrin and non-integrin receptors. One of the non-integrin receptors is the mw 67K laminin receptor, LBP [19]. A highly conserved multifunctional mw 37K laminin receptor protein is the precursor of the 67K laminin receptor but the exact manner by which it forms a mature laminin receptor is not clear [20]. Endo and co-workers demonstrated that the glycans of α-dystroglycan include *O*-mannosyl oligosaccharides,

and that a sialyl *O*-mannosyl glycan, Siaα 2,3Galβ1,4GlcNAcβ1,2Man, of α-dystroglycan is a laminin-binding ligand of α-dystroglycan [21,22]. Furthermore, α-dystroglycan from sheep brain has an SSEA-1 structure O-linked to Man [23]. We found that another non-integrin laminin receptor, LBP of human and mouse EC cells, has the SSEA-4 epitope. Since laminin is essential to autocrine- or paracrine-signaling throughout mammalian development and differentiation, the up-regulation of laminin production might have some relationship with SSEA-4 expression on the laminin receptor. However, Raft.2 had no significant effects on F9 cell adhesion to a coverslip precoated with the murine Engelbreth–Holm–Swam tumor-derived laminin (data not shown).

The F9 cell exhibits a distinct pattern of globo- and neolacto-series oligosaccharide chain elongation (Fig. 7). In the globoseries pathway, globotetraosylceramide (Gb4) is not elongated to globopentaosylceramide (Gb5) by the addition of Gal, but rather to the Forssman antigen by the addition of GalNAc [24]. The β1,3-galactosyltransferase-V (β3GalT-V) can catalyze the transfer of Gal not only to GlcNAc-based acceptors with a preference for the core3 O-linked glycan GlcNAc(β1,3)-GalNAc structure, but also to the terminal GalNAc unit of Gb4, thereby leading to the synthesis of Gb5 [25]. These investigators further confirmed that Gb5 synthesis, or SSEA-3 expression in F9 cells is due to β3GalT-V. SSEA-3 synthase, i.e., β3GalT-V, can be said to catalyze Gal addition to both the acceptor of glycolipid and protein. SSEA-4 synthase, which transfers sialic acid to Gb5, was recently cloned from a human renal cancer cell line, ACHN, and the cloned cDNA was found to have a sequence identical to previously cloned α2,3-sialyltransferase (ST3Gal II) [26]. It catalyzes the transfer of sialic acid to the Galβ1,3GalNAc epitope of Gb5 in addition to asialo-GM1 and GM1a [27]. Whether ST3Gal II acts on a proteinous acceptor, such as LBP, is unknown. These transferases, which can glycosylate LBP, should be characterized to elucidate the role of the sugar moiety in differentiation.

Acknowledgments

We thank Ms. S. Yamauchi for her excellent secretarial work, and Drs. Susumu Watanabe and Tomomi Kayamori of Hitachi Science Systems, for mass spectrometric analysis of the Raft.2-binding protein. This work was supported in part by MEXT. KAKENHI 16017321, a grant from the Japan Health Sciences Foundation for Research on Health Sciences Focusing on Drug Innovation KH21014 and also by the CREST grant from the Japan Science and Technology.

References

[1] L.H. Shevinsky, B.B. Knowles, I. Damjanov, D. Solter, Monoclonal antibody to murine embryos defines a stage-specific embryonic antigen expressed on mouse embryos and human teratocarcinoma cells, Cell 30 (1982) 697–705.

[2] N.W. Fox, I. Damjanov, B.B. Knowles, D. Solter, Stage-specific embryonic antigen 3 as a marker of visceral extraembryonic endoderm, Dev. Biol. 103 (1984) 263–266.

[3] P.W. Andrews, Retinoic acid induces neuronal differentiation of a cloned human embryonal carcinoma cell line in vitro, Dev. Biol. 103 (1984) 285–293.

[4] R. Kannagi, E. Nudelman, S.B. Levery, S. Hakomori, A series of human erythrocyte glycosphingolipids reacting to the monoclonal antibody directed to a developmentally regulated antigen SSEA-1, J. Biol. Chem. 257 (1982) 14865–14874.

[5] R. Kannagi, N.A. Cochran, F. Ishigami, S. Hakomori, P.W. Andrews, B.B. Knowles, D. Solter, Stage-specific embryonic antigens (SSEA-3 and -4) are epitopes of a unique globo-series ganglioside isolated from human teratocarcinoma cells, EMBO J. 2 (1983) 2355–23561.

[6] Y.U. Katagiri, K. Ohmi, C. Katagiri, T. Sekino, H. Nakajima, T. Ebata, N. Kiyokawa, J. Fujimoto, Prominent immunogenicity of monosialosyl galactosylgloboside, carrying a stage-specific embryonic antigen-4 (SSEA-4) epitope in the ACHN human renal tubular cell line-a simple method for producing monoclonal antibodies against detergent-insoluble microdomains/raft, Glycoconj. J. 18 (2001) 347–353.

[7] T. Maruyama, A. Umezawa, S. Kusakari, H. Kikuchi, M. Nozaki, J. Hata, Heat shock induces differentiation of human embryonal carcinoma cells into trophectoderm lineages, Exp. Cell Res. 224 (1996) 123–127.

[8] K. Nakamura, M. Suzuki, C. Taya, F. Inagaki, T. Yamakawa, A. Suzuki, A sialidase-susceptible ganglioside, IV3 alpha(NeuGc alpha 2-8NeuGc)-Gg4Cer, is a major disialoganglioside in WHT/Ht mouse thymoma and thymocytes, J. Biochem. 110 (1991) 832–841.

[9] H. Nakajima, Y.U. Katagiri, N. Kiyokawa, T. Taguchi, T. Suzuki, T. Sekine, K. Mimori, H. Nakao, T. Takeda, J. Fujimoto, Single-step method for purification of Shiga toxin-1 B subunit using receptor-mediated affinity chromatography by globotriaosylceramide-conjugated octyl sepharose CL-4B, Protein Exp. Purif. 22 (2001) 267–275.

[10] Y.U. Katagiri, K. Ohmi, W. Tang, H. Takenouchi, T. Taguchi, N. Kiyokawa, J. Fujimoto, Raft.1, a monoclonal antibody raised against the raft microdomain, recognizes G-protein β1 and 2, which assemble near nucleus after Shiga toxin binding to human renal cell line, Lab. Invest. 82 (2002) 1735–1745.

[11] K. Nakamura, Y. Hashimoto, M. Suzuki, A. Suzuki, T. Yamakawa, Characterization of GM1b in mouse spleen, J. Biochem. 96 (1984) 949–957.

[12] R. Kannagi, S.B. Levery, F. Ishigami, S. Hakomori, L.H. Shevinsky, B.B. Knowles, D. Solter, New globoseries glycosphingolipids in human teratocarcinoma reactive with the monoclonal antibody directed to a developmentally regulated antigen, stage-specific embryonic antigen 3, J. Biol. Chem. 258 (1983) 8934–8942.

[13] M. Ozawa, T. Muramatsu, D. Solter, SSEA-1, a stage-specific embryonic antigen of the mouse, is carried by the glycoprotein-bound large carbohydrate in embryonal carcinoma cells, Cell Differ. 16 (1985) 169–173.

[14] J.K. Henderson, J.S. Draper, H.S. Baillie, S. Fishel, J.A. Thomson, H. Moore, P.W. Andrews, Preimplantation human embryos and embryonic stem cells show comparable expression of stage-specific embryonic antigens, Stem Cells 20 (2002) 329–337.

[15] A. van de Stolpe, M. Karperien, C.W. Lowik, H. Juppner, G.V. Segre, A.B. Abou-Samra, S.W. de Laat, L.H. Defize, Parathyroid hormone-related peptide as an endogenous inducer of parietal endoderm differentiation, J. Cell Biol. 120 (1993) 235–243.

[16] K.M. Malinda, K.H. Kleinman, The laminins, Int. J. Biochem. Cell Biol. 28 (1996) 957–959.

[17] K.M. Malinda, M. Nomizu, M. Chung, M. Delgado, Y. Kuratomi, Y. Yamada, H.K. Kleinman, M.L. Ponce, Identification of laminin alpha1, and beta1 chain peptides active for endothelial cell adhesion, tube formation, and aortic sprouting, FASEB J. 13 (1999) 53–62.

[18] J.H. Miner, P.D. Yurchenco, Laminin functions in tissue morphogenesis, Annu. Rev. Cell Dev. Biol. 20 (2004) 255–284.

[19] E.E. Simon, J.A. McDonald, Extracellular matrix receptors in the kidney cortex, Am. J. Physiol. 259 (1990) F783–F792.

[20] S. Buto, E. Tagliabue, E. Ardini, A. Magnifico, C. Ghirelli, F. van den Brule, V. Castronovo, M.L. Colnaghi, M.E. Sobel, S. Menard, Formation of the 67-kDa laminin receptor by acylation of the precursor, J. Cell. Biochem. 69 (1998) 244–251.

[21] A. Chiba, K. Matsumura, H. Yamada, T. Inazu, T. Shimizu, S. Kusunoki, I. Kanazawa, A. Kobata, T. Endo, Structures of sialylated O-linked oligosaccharides of bovine peripheral nerve alpha-dystroglycan. The role of a novel O-mannosyl-type oligosaccharide in the binding of alpha-dystroglycan with laminin, J. Biol. Chem. 272 (1997) 2156–2162.

[22] T. Sasaki, H. Yamada, K. Matsumura, T. Shimizu, A. Kobata, T. Endo, Detection of O-mannosyl glycans in rabbit skeletal muscle alpha-dystroglycan, Biochim. Biophys. Acta 1425 (1998) 599–606.

[23] N.R. Smalheiser, S.M. Haslam, M. Sutton-Smith, H.R. Morris, H.R.A. Dell, Structural analysis of sequences O-linked to mannose reveals a novel Lewis X structure in cranin (dystroglycan) purified from sheep brain, J. Biol. Chem. 273 (1998) 23698–23703.

[24] J.G. Krupnick, I. Damjanov, A. Damjanov, Z.M. Zhu, B.A. Fenderson, Globo-series carbohydrate antigens are expressed in different forms on human and murine teratocarcinoma-derived cells, Int. J. Cancer 59 (1994) 692–698.

[25] D. Zhou, T.R. Henion, F.B. Jungalwala, E.G. Berger, T. Hennet, The beta 1,3-galactosyltransferase beta 3GalT-V is a stage-specific embryonic antigen-3 (SSEA-3) synthase, J. Biol. Chem. 275 (2000) 22631–22634.

[26] S. Saito, H. Aoki, A. Ito, S. Ueno, T. Wada, K. Mitsuzuka, M. Satoh, Y. Arai, T. Miyagi, Human alpha2,3-sialyltransferase (ST3Gal II) is a stage-specific embryonic antigen-4 synthase, J. Biol. Chem. 278 (2003) 26474–26479.

[27] Y.J. Kim, K.S. Kim, S.H. Kim, C.H. Kim, J.H. Ko, I.S. Choe, S. Tsuji, Y.C. Lee, Molecular cloning and expression of human Gal beta 1,3GalNAc alpha 2,3-sialytransferase (hST3Gal II), Biochem. Biophys. Res. Commun. 228 (1996) 324–327.

Cell Separation Between Mesenchymal Progenitor Cells Through Porous Polymeric Membranes

Akon Higuchi,[1] Yosuke Shindo,[1] Yumiko Gomei,[1] Taisuke Mori,[2] Taro Uyama,[2] Akihiro Umezawa[2]

[1]Department of Applied Chemistry, Seikei University, 3-3-1 Kichijoji Kitamachi, Musashino, Tokyo 180-8633, Japan

[2]Department of Reproductive Biology and Pathology, National Center for Child and Development, Setagaya, Tokyo 154-8567

Received 9 August 2004; revised 5 October 2004; accepted 12 October 2004
Published online 19 May 2005 in Wiley InterScience (www.interscience.wiley.com). DOI: 10.1002/jbm.b.30220

Abstract: This study investigates the separation of two types of marrow stromal cells, KUSA-A1 osteoblasts and H-1/A preadipocytes, by filtration through various porous polymeric membranes. It was found that KUSA-A1 permeates better than H-1/A cells through 12-μm polyurethane foaming membranes. This appears to be due to the relatively smaller cell size of KUSA-A1 cells. In addition, when feed solutions containing suspensions of either cell type or a mixture of the two were used, the permeation ratio was relatively low (< 6%) through polyurethane and surface-modified polyurethane foaming membranes. It was also found that there was some degree of separation between KUSA-A1 and H-1/A cells (separation factor = 1.8) with nylon-net filter membranes, but no separation was obtained when filters made of nonwoven fabrics or silk screens were used. This ability of the nylon-net filter membranes to separate the two cell types was due to a sieving effect that results from an optimal pore size. Finally, permeation of a solution of human serum albumin through the membrane following filtration of the cells did not result in a separation of cells in the recovery solution. © 2005 Wiley Periodicals, Inc. J Biomed Mater Res Part B: Appl Biomater 74B: 511–519, 2005

Keywords: cell separation; mesenchymal progenitor cells; flow cytometry; biomaterials; polyurethane foaming membrane

INTRODUCTION

Bone-marrow stromal cells make up the microenvironment of the bone marrow and are required for the generation of multipotent stem cells.[1] In addition, bone-marrow stromal cells have many characteristics of mesenchymal stem cells, which produce progeny that can differentiate into multiple cell lineages. Pluripotent stem cells derived from marrow stroma can differentiate into several cell types, including bone, cartilage, fat, tendon, and muscle. Recent studies also show that the marrow stroma may be a potential source of cardiomyocytes.[2]

Purification and isolation of specific mesenchymal cells are necessary to obtain bone-marrow stromal cells for use in clinical applications. For example, it is necessary to generate cardiomyocytic progenitors from marrow stroma for the treatment of heart failure by cell transplantation into damaged myocardia. Thus, a method is needed for the separation and isolation of specific mesenchymal cells from bone-marrow stromal cells. Cell separation can be accomplished by centrifugation,[3,4] fluorescence-activated cell sorting (FACS),[5] magnetic cell selection,[6–9] affinity chromatography,[10,11] or membrane filtration.[12–14] Of these methods, membrane filtration method is a good candidate for the purification of mesenchymal cells because it is simple and inexpensive and because it is easy to maintain sterility during the filtration process. In fact, a previous study[14] showed that $CD34^+$ cells could be purified by filtration through chemically modified 5-μm-pore polyurethane (PU) membranes.

Here the separation of cells from a mixture of KUSA-A1 and H-1/A cells with the use of membrane filtration is reported. The goal of this study was to find the optimal membrane type (membrane pore size, morphology, and material) and filtration conditions for the isolation of marrow stromal cells.

MATERIALS AND METHODS

Materials

Base membranes used for the chemical modification were porous PU foaming membranes (Ruby Cell S, Toyo Polymer Co., Ltd.). Porous PU foaming membranes containing 0.61% of epoxy group (PU-epoxy) were prepared by plasma polymerization with glycidylmethacrylate after the membranes were plasma discharged at 200 W for 30 s under 0.2 torr of Ar gas.[14] The average pore size of the PU

Correspondence to: Akno Higuchi (e-mail: higuchi@ch.seikei.ac.jp)
Contract grant sponsor: Ministry of Education, Culture, Sports, Science, and Technology of Japan Grant-in-Aid for Scientific Research on Priority Areas (B, "Novel Smart Membranes Containing Controlled Molecular Cavity"); contract grant number: 13133202
Contract grant sponsor: Salt Science Foundation
Contract grant sponsor: Asahi Glass Foundation

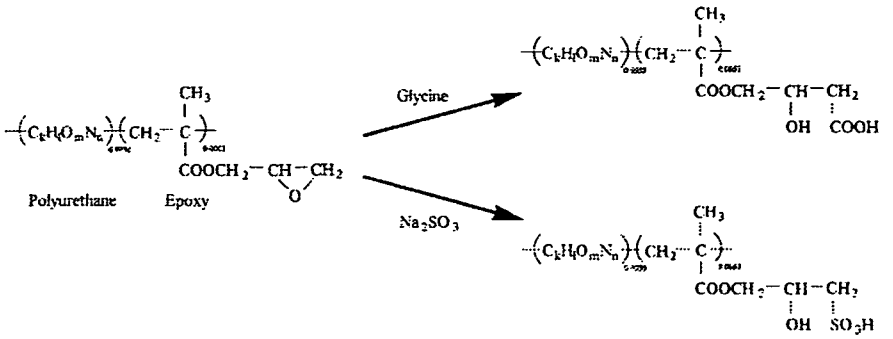

Scheme 1

and PU-epoxy membranes evaluated from capillary flow porometer measurements (Porous Materials, Inc.) was 12 μm. The PU and PU-epoxy membranes had 86% porosity and 1.2-mm thickness.

Nylon-net filters [NY11 (pore size = 11 μm), Millipore Corporation], two kinds of nonwoven fabrics having fine fiber diameter for cleaning lenses made of acrylonitrile (Cleaning lens, No Brand Co.) and nylon + polyester (La Clean, 3052-01, Nagoya Glass Co.), and silk screens made of silk (No. 150, Nihon Zokei Co.) and Tetron™ (Nos. 150 and 250, Nihon Zokei Co.) were also used for the cell separation, where "No." indicates number of fibers per inch.

Human serum albumin (HSA, 019-10503, Wako Pure Chemical Industries) was used as received. Cell Tracker Orange™ (C-2927, Molecular Probes, Inc.) and Cell Tracker Green™ (C-2925, Molecular Probes, Inc.) were used as received. Other chemicals, purchased from Tokyo Chemical Co., were reagent grade and were used without further purification. Ultrapure water was used throughout the experiments.

Preparation of Surface-Modified Membranes

Sulfonic acid and carboxylic acid groups were introduced from the opening reaction of the epoxy group on the PU-epoxy membranes, followed by the reaction between the epoxy group and H_2SO_4 or glycine reported in the literature.[14–16] Reaction conditions are reported in the literature.[14] The product anticipated to result from the ring-opening reaction of the epoxy group is shown in Scheme 1.[14] The resultant membranes were referred to as PU-SO_3H and PU-COOH membranes. After the reaction, the surface-modified PU membranes were rinsed in ultrapure water for 3 h, and stocked in ultrapure water at 4°C.

Cell Culture

Mesenchymal progenitor cell lines, KUSA-A1 and H-1/A, derived from the bone marrow of C3H/He and C57/Bl mice, respectively,[1,2] were maintained in DMEM media (D5648, Sigma-Aldrich, Japan K.K.) supplemented with 100 mg/L streptomycin sulfate (196-08511, Wako Pure Chemical Industry, Ltd.), 70 mg/L benzylpenicillin potassium (023-07731, Wako Pure Chemical Industry, Ltd.) and 10% fetal bovine serum (FBS, JRH Bioscience). KUSA-A1 and H-1/A cells were expanded by standard cell culture techniques[17–19] in 75-cm^2 tissue-culture flasks containing 40 mL of 10% serum-supplemented medium in a CO_2 incubator (BNA-111, Espec Co.) in 5% CO_2 atmosphere at 37°C.

The cell number was characterized by observation of the cells with an inverted microscope (Diaphoto TMD300, Nikon Co.) equipped with a CCD video camera, ARGUS 20 (Hamamatsu Photonics K.K.) and a temperature-regulated box.

Cell Dying with Cell Tracker

KUSA-A1 cells and H-1/A cells were dyed with Cell Tracker™ (Cell Tracker Orange™ and Cell Tracker Green™, respectively) in order to mark each cell in flow-cytometry analysis. A quantity of 1 mg Cell Tracker Orange™ was dissolved in 1 mL of methanol, and the Cell Tracker Orange™ solution was aliquotted into 20 samples (50 μL). A quantity of 50 μg Cell Tracker Green™ was dissolved in 0.5 mL of dimethylsulfoxide, and the Cell Tracker Green™ solution was aliquotted into 10 samples (50 μL). The Cell Tracker Orange™ and Cell Tracker Green™ solutions were stored under −20°C. The cell dying with Cell Tracker Orange™ and Cell Tracker Green™ was performed as follows:

1. A quantity of 50 μL of Cell Tracker solution was pipetted into 5 mL of 10% serum-supplemented DMEM medium.
2. The medium was decanted off, and the cells were rinsed with 10 mL phosphate-buffered solution (PBS).
3. The PBS was decanted off and the Cell Tracker™ solution was pipetted into the tissue-culture flask. The cells in the tissue-culture flask were incubated in a 5% CO_2 atmosphere for 30 min at 37°C.
4. The Cell Tracker™ medium was decanted off and the cells were subsequently rinsed with a quantity of 10 mL PBS solution. Twenty milliliters of 10% serum-supplemented DMEM medium was pipetted into the tissue-culture flask after the PBS solution was decanted off, and the cells in the tissue-culture flask were again incubated in a 5% CO_2 atmosphere for 30 min at 37°C.
5. Step 4 was performed in duplicate.
6. After incubation, the DMEM medium was decanted off and a quantity of 10 mL PBS solution was added to the tissue-culture flask in order to rinse the cells.
7. A quantity of 4 mL of trypsin in PBS solution was pipetted into the tissue-culture flask after the PBS solution was decanted off. After 5 min, the trypsin solution was decanted off and a quantity of 5 mL of DMEM medium was added to the tissue-culture flask. The cells on the bottom of the culture flask were resuspended in the DMEM medium by gently pipetting up and down.
8. The cell suspension was centrifuged at 130 rpm for 3 min. The supernatant was carefully decanted off, and 7 mL of fresh DMEM medium was added to the cells.

9. The cell suspension was gently pipetted up and down to resuspend cells on the bottom of the centrifuge tube, and the cell density was counted with the use of flow cytometry (Coulter EPICS™ XL, Beckman-Coulter Co.).

Cell Permeation

KUSA-A1 cells and H-1/A cells were inserted into the centrifugation tube containing DMEM medium. Each cell density was adjusted to be 50,000 cells/mL by the addition of DMEM medium. The single- or mixed-cell solution of 6 mL containing KUSA-A1 cells and/or H-1/A cells was permeated through the membranes with the permeation apparatus described in the previous study.[14] The diameter of the membrane was 25 mm and filtration rate was 1 mL/min. The number of each cell of KUSA-A1 cells and H-1/A cells in the permeate and feed solutions (N_p and N_f, respectively) was counted from the flow-cytometry measurements.

The permeation ratio is defined as

$$\text{permeation ratio } (\%) = (N_p/N_f) \times 100. \quad (1)$$

After the cell filtration, the membrane was upside down inside the membrane holder, and 0.5-wt % HSA solution of 6 mL was permeated through the membrane with the use of the same membrane and the apparatus at filtration speed of 1 mL/min to remove the attached cells on the membrane and to collect them in the HSA solution. The recovery ratio is defined as

$$\text{recovery ratio } (\%) = (N_r/N_f) \times 100, \quad (2)$$

where N_r is the number of cells in the permeate solution after the permeation of HSA solution. The filtration experiments were performed at 25±0.5°C.

The membranes used in the cell filtration were unmodified PU membranes, surface-modified PU membranes, nylon-net filters, nonwoven fabrics, and silk screens. The permeation experiments of cells were performed on each membrane with four independent membranes.

Flow-Cytometric Analysis of Cells

The size and shape of KUSA-A1 cells and H-1/A cells were analyzed from forward light scattering and side light scattering of laser beam (Ar laser, 488 nm) by flow cytometry. The number of KUSA-A1 cells and H-1/A cells in the feed and permeate solutions was analyzed from flow-cytometric scattergrams of KUSA-A1 cells and H-1/A cells in the fluorescent intensity at 575 and 525 nm.

SEM Analysis of Cells on the Membranes

After permeation of suspended cell solution through the membranes, the membranes were rinsed with saline. Consequently, the membranes were treated with 3-wt % glutaraldehyde in saline for 2 days at 4°C. The samples were washed with saline, subjected to a drying process by being passed through a series of graded-alcohol–saline solutions (0, 25, 50, 75, and 100%) and dried in a vacuum for 10 h at room temperature.[20] The dried membranes were gold coated and examined with the use of a JSM-5200 scanning electron microscope (SEM, JEOL, Ltd.).

RESULTS AND DISCUSSION

Flow-Cytometric Analysis of Cells

KUSA-A1 osteoblasts and H-1/A preadipocytes, two mesenchymal cell lines, were incubated with fluorescent probes (Cell Tracker Orange™ and Cell Tracker Green™, respectively) to allow their independent detection before and after permeation through porous polymeric membranes. The numbers of KUSA-A1 and H-1/A cells in the mixed cell solution were determined from flow-cytometric scattergrams at 575 nm for KUSA-A1 cells and 525 nm for H-1/A cells. These values are close to those of phycoerythrin (PE) and fluorescein isothiocyanate (FITC), which are used for conventional cell-counting of specific cells.[21] Figure 1(a) shows the flow-cytometric scattergrams for the KUSA-A1 and H-1/A cells. The fluorescence intensities at 525 and 575 nm for the two cell types were significantly different. The forward and side light scattering intensities, shown in Figure 1(b), indicate that both cell types have a broad size distribution, although KUSA-A1 cells are mostly smaller than H-1/A cells. Furthermore, the flow-cytometric scattergrams of KUSA-A1 cells and H-1/A cells (forward light scattering intensity vs. side light scattering intensity and fluorescence intensity at 525 nm vs. 575 nm) were found to be identical in single- and mixed-cell solutions (data not shown). Thus, cell aggregates did not appear to be formed when KUSA-A1 cells and H-1/A cells were mixed together in DMEM medium.

Cell Separation Through PU Membranes

The differences in the cell sizes and shapes suggested that KUSA-A1 and H-1/A cells can be separated by using porous polymeric membranes. This possibility was examined with the use of a variety of membrane types. Figure 2 shows an SEM image of the surface of the porous polymeric membranes tested in this study. A regular screen pore morphology was found on the surface of nylon-net filters [Figure 2(b)] and silk screens [Figure 2(e,f)], whereas a specific pore morphology was not found on the surface of nonwoven fabrics [Figure 2(c,d)]. Furthermore, a deformed open pore structure was found on the surface of the PU membranes used in this study [Figure 2(a)].

The permeation of cells through PU and surface-modified PU membranes was investigated first, because a previous study showed that hematopoietic stem cells can be recovered from peripheral blood with the use of surface-modified PU (PU-COOH) membranes.[14] The permeation of KUSA-A1 cells, H-1/A cells, and a mixture of the two cell types through PU and surface-modified PU membranes (pore size = 12 μm) at 25°C was examined. Figure 3(a) shows the permeation ratio through the membranes with a suspension of a single cell type (50,000 cells/mL) used as the feed solution, and Figure 4(a) shows the results obtained when the feed solution was a mixture of the two cell types. A relatively low (< 6%) permeation ratio through PU and surface-modified PU membranes was found with either a single-cell solution or a mixed-cell solution. Because open pore volume of the

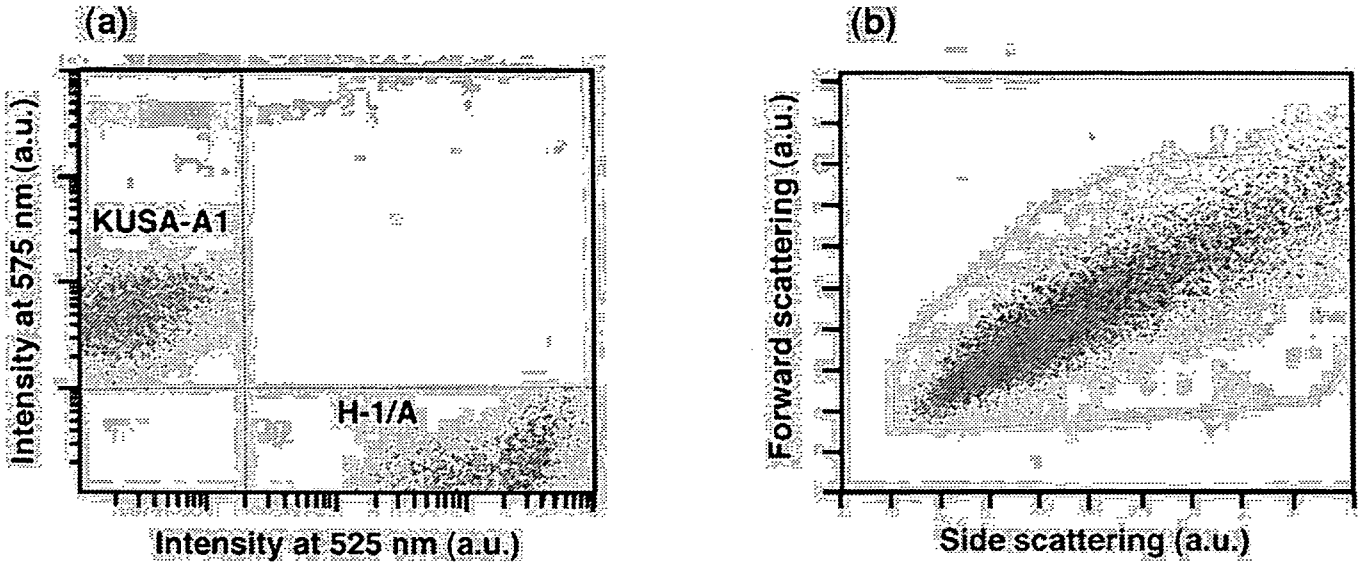

Figure 1. Flow-cytometric scattergrams of mixed solution of KUSA-A1 cells (orange dots) and H-1/A cells (green dots), each having a cell density of 50,000 cells/mL in the fluorescent intensity at 575 nm and 525 nm (a) and in the light intensity of forward scattering and side scattering (b). [Color figure can be viewed in the online issue, which is available at www.interscience.wiley.com.]

membrane interior in PU and surface-modified PU membranes is calculated as 0.506 mL (i.e., 1.25 cm × 1.25 cm × 3.14 × 0.12 cm × 0.86) and total cell volume permeated through the membranes is approximately calculated as 3.375×10^{-4} mL in a mixed-cell solution [i.e., 6 mL × 50,000 cells/mL × 2 × (7.5×10^{-4} cm × 7.5×10^{-4} cm ×

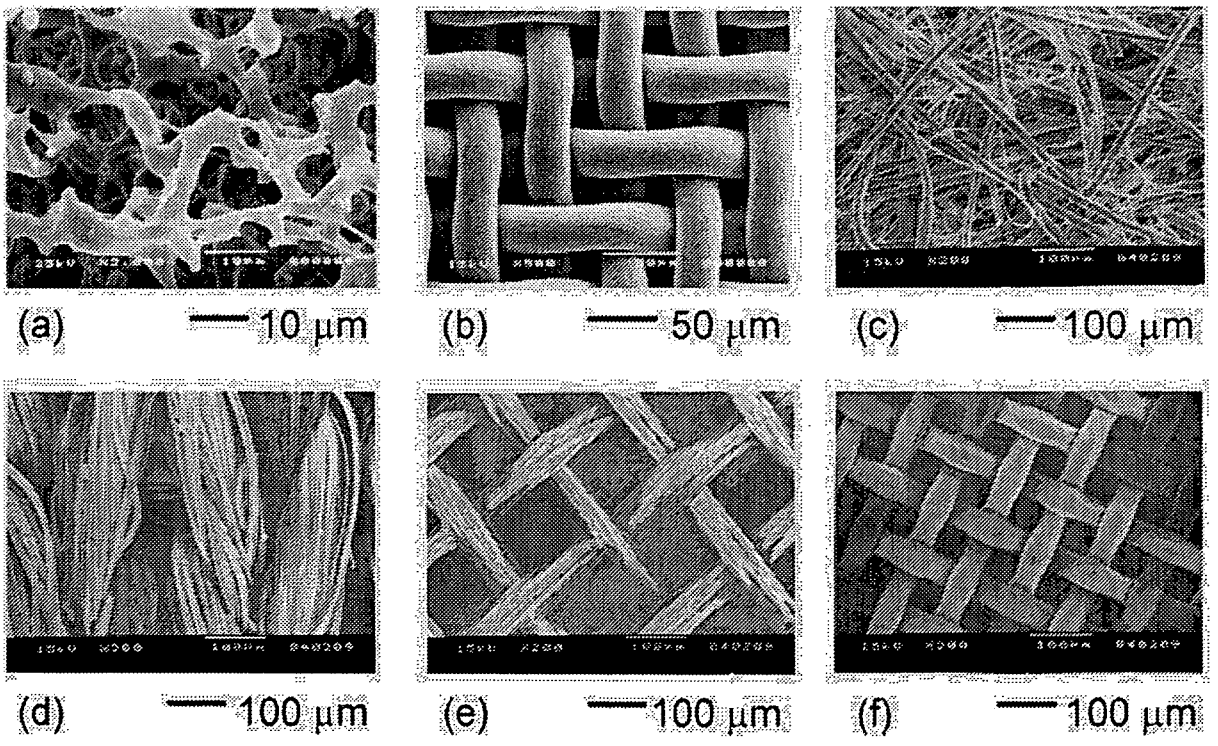

Figure 2. Scanning electron micrographs of the membrane surfaces of (a) unmodified PU membranes, (b) nylon-net filter, (c) nonwoven fabrics made of acrylonitrile, (d) nylon + polyester, (e) silk screens made of silk mesh size 150), and (f) silk screens made of Tetron™ (mesh size 250).

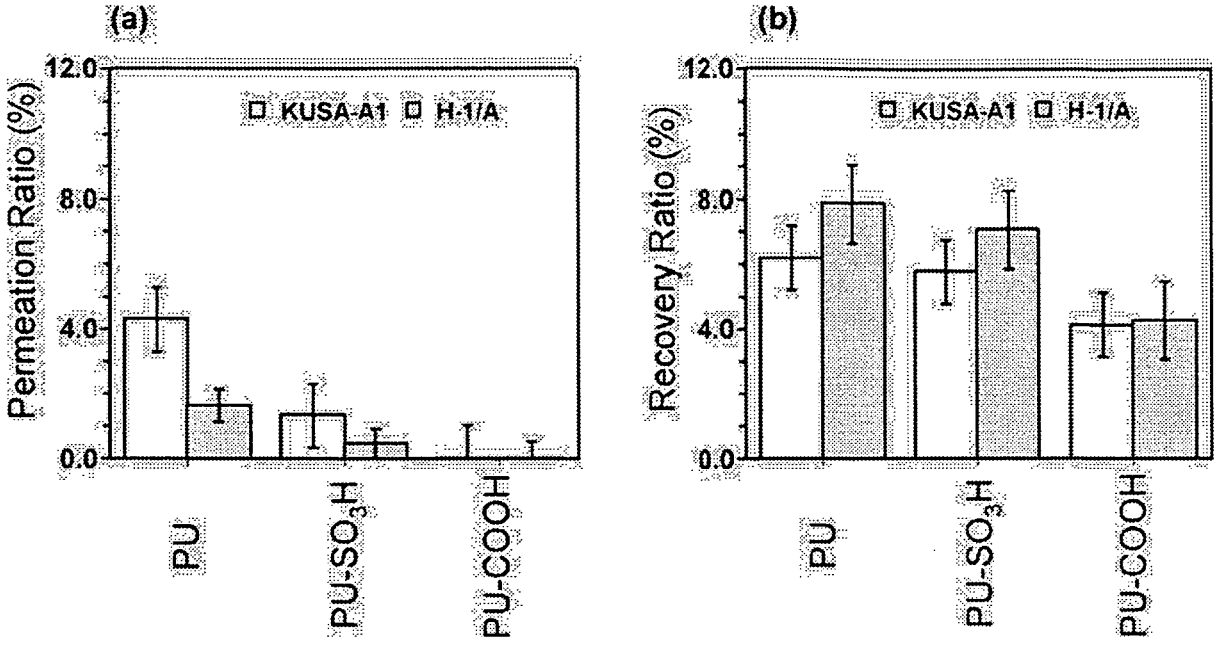

Figure 3. Permeation ratio (a) and recovery ratio (b) of KUSA-A1 cells and H-1/A cells through PU, PU-SO_3H, and PU-COOH membranes after permeation of single-cell solution at the cell density of 50,000 cells/mL and 25°C. Data are expressed as the means ± standard deviation of four independent measurements.

7.5×10^{-4} cm × 4/3)] in this study, the low permeation ratio is not due to the overloading of the cells permeated through the membranes. The low permeation ratio through PU and surface-modified PU membranes is due to high degree of cell adhesion on the membranes and a complicated pore structure of the membranes.

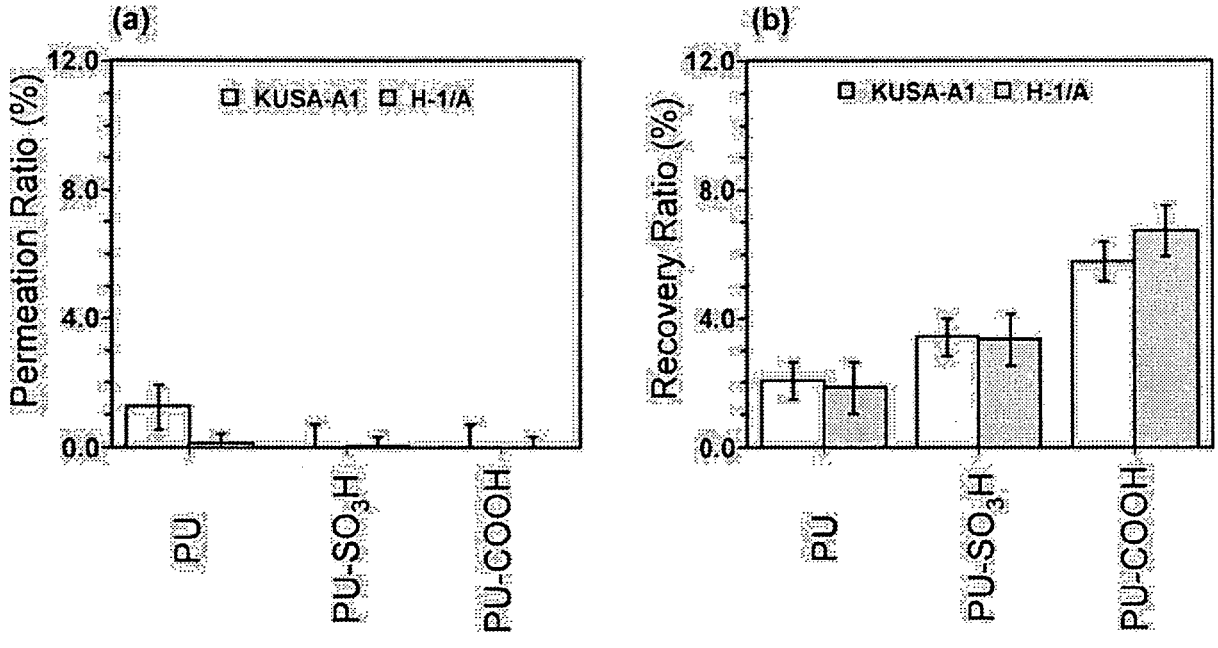

Figure 4. (a) Permeation ratio and (b) recovery ratio of KUSA-A1 cells and H-1/A cells through PU, PU-SO_3H, and PU-COOH membranes after permeation of mixed-cell solution at a cell density of 50,000 cells/mL each and 25°C. Data are expressed as the means ± standard deviation of four independent measurements.

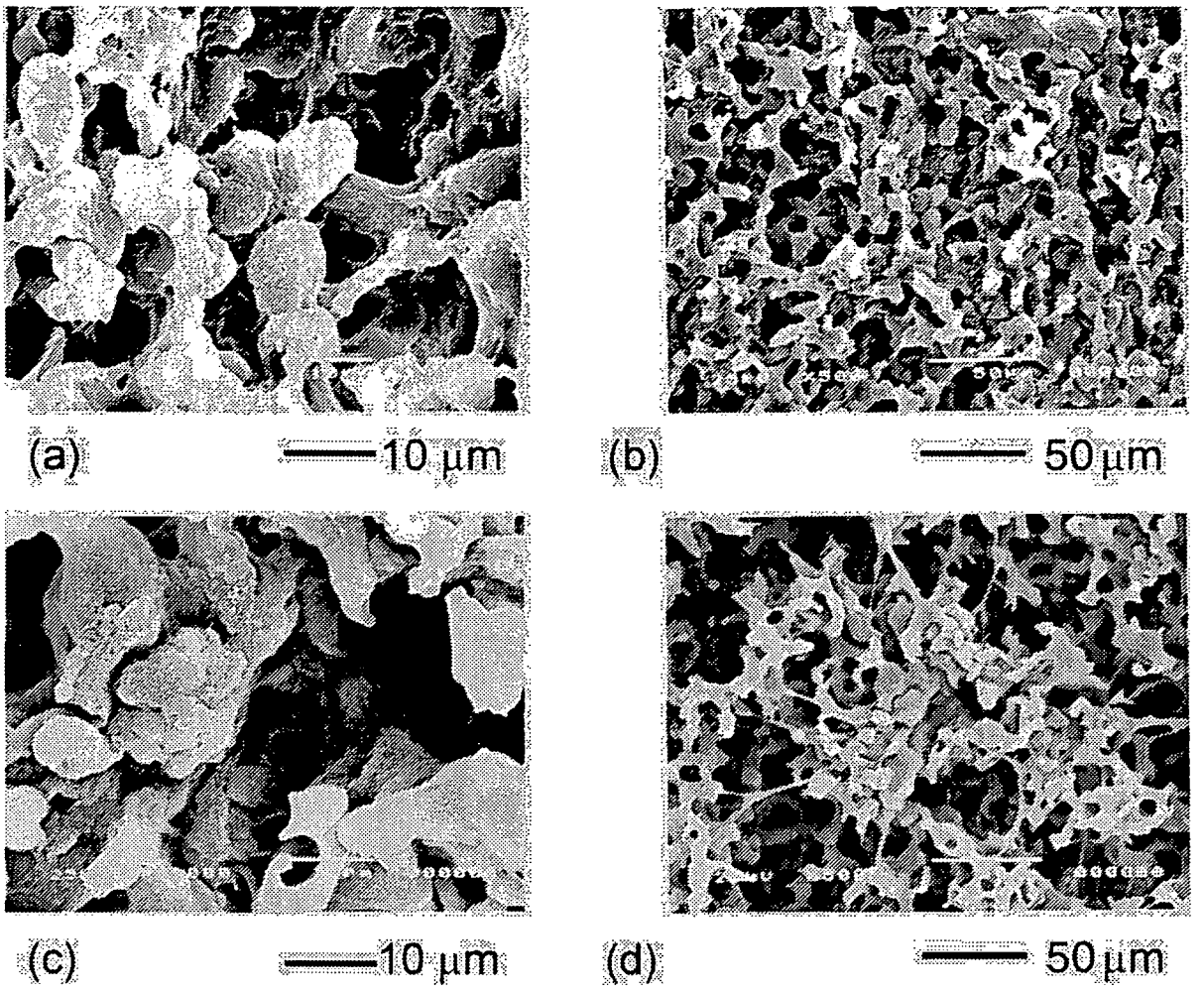

Figure 5. Scanning electron micrograph of membrane surface of unmodified PU membranes after permeation of KUSA-A1 cells (a), (b) or H-1/A cells (c), (d) at the cell density of each 50,000 cells/mL and 25°C.

The permeation ratio of both KUSA-A1 and H-1/A cells through PU membranes was found to be higher than that through PU-SO_3H and PU-COOH membranes. The surface modification of PU-SO_3H and PU-COOH membranes may cause the decreased pore size of the surface-modified membranes compared to the unmodified PU membranes. The permeation ratio when the feed solution contained a single cell type was found to be higher than the permeation ratio when it was a mixed-cell solution through PU and surface-modified PU membranes. Although FACS analysis suggested that coagulation or interaction does not occur between KUSA-A1 and H-1/A cells (data not shown), some coagulation or interaction between KUSA-A1 and H-1/A cells that was not detected from FACS analysis might lead to a decrease of the permeation ratio in the mixed-cell solution compared to the permeation ratio in the single-cell solution. It was also found that the permeation ratio for KUSA-A1 cells was higher than for H-1/A cells, which is consistent with the relatively smaller size of KUSA-A1 cells, as found in Figure 1(b).

Figure 5 shows a SEM image of the PU membrane surface after the permeation of KUSA-A1 or H-1/A cells. There was extensive adhesion of the KUSA-A1 and H-1/A cells to the membrane surface. The high adhesiveness of the cells may explain their low permeation ratios through the PU membranes. SEM images also revealed that the size of KUSA-A1 cells was similar to that of H-1/A cells (approximately 10 to 15 μm in diameter).

Next the effect of passing a HSA solution through the membranes following permeation of the single-cell or mixed-cell solutions was examined. Figures 3(b) and 4(b) show that the recovery ratio of KUSA-A1 and H-1/A cells following this treatment was higher than the permeation ratio. However, the recovery ratio was still below 10% through any of the PU membranes. Slightly higher recovery ratio through the PU and PU-SO_3H membranes in a mixed feed solution was found when compared to that in a single-cell type. On the other hand, no significant difference in recovery ratio was found between feed solutions containing a single cell type or a mixture of cell types through PU-COOH membranes.

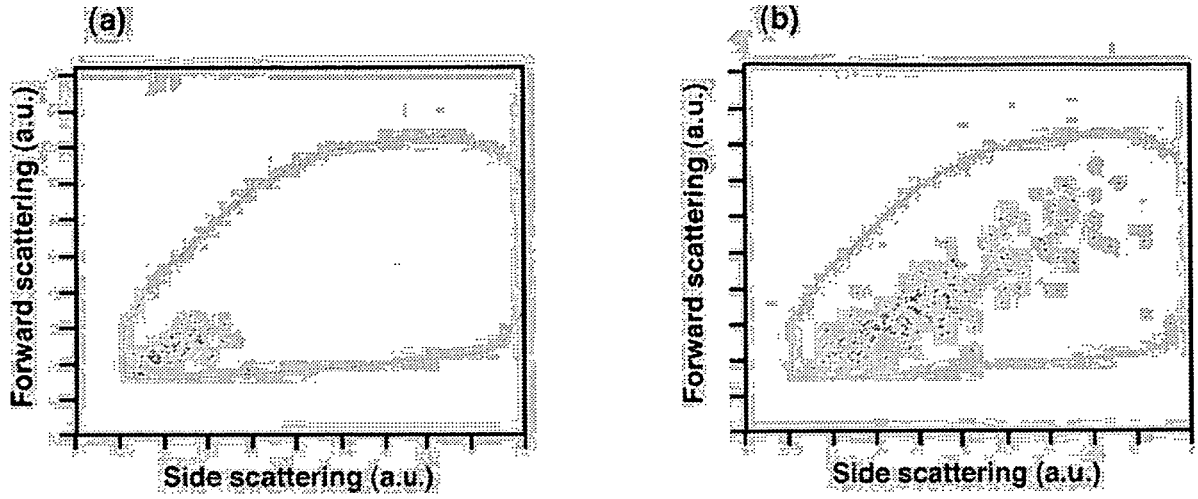

Figure 6. Flow-cytometric scattergrams of KUSA-A1 cells (orange dots) and H-1/A cells (green dots) in the relationship between forward light scattering intensity and side light scattering intensity in the permeate solution after permeation of mixed cells of KUSA-A1 cells (orange dots) and H-1/A cells (green dots) through the PU membranes at (a) the cell density of each 50,000 cells/mL, and (b) following subsequent permeation of HSA solution. [Color figure can be viewed in the online issue, which is available at www.interscience.wiley.com.]

Next the flow-cytometric analysis of the permeate solution of KUSA-A1 and H-1/A cells and also that of the recovery solution following filtration through PU membranes were examined. Figure 6(a) shows the forward versus side light scattering intensity in the permeate solution after permeation of the cells through PU membranes. Both smaller-sized KUSA-A1 and H-1/A cells passed through the PU membranes. Therefore, KUSA-A1 cells have a higher permeation ratio than H-1/A cells, because KUSA-A1 cells are typically smaller than H-1/A cells (see Figure 1).

Figure 6(b) shows the results of recovery solution following subsequent permeation of HSA solution. The pattern of the scattergram in the recovery solution [Figure 6(b)] was identical to that of the feed solution [Figure 1(b)], even though the numbers of both KUSA-A1 cells and H-1/A cells were significantly lower in the recovery solution. Thus, there is not a significant separation of KUSA-A1 and H-1/A cells in the recovery solution following permeation with HSA solution.

Cell Separation Through Various Porous Membranes

The separation of KUSA-A1 and H-1/A cells by several porous membranes, including uncoated nylon-net filters, fibronectin- or collagen-coated nylon-net filters, nonwoven fabrics made of acrylonitrile or a combination of nylon and polyester, silk screen No. 150 made of silk or Tetron™, and silk screen No. 250 made of Tetron™ were also examined. Figure 7 shows the permeation ratio through these membranes with the use of a feed solution containing a mixture of KUSA-A1 and H-1/A cells. With the use of the nylon-net filter and fibronectin-coated nylon-net filter, the permeation ratio for KUSA-A1 cells was higher than for H-1/A cells.

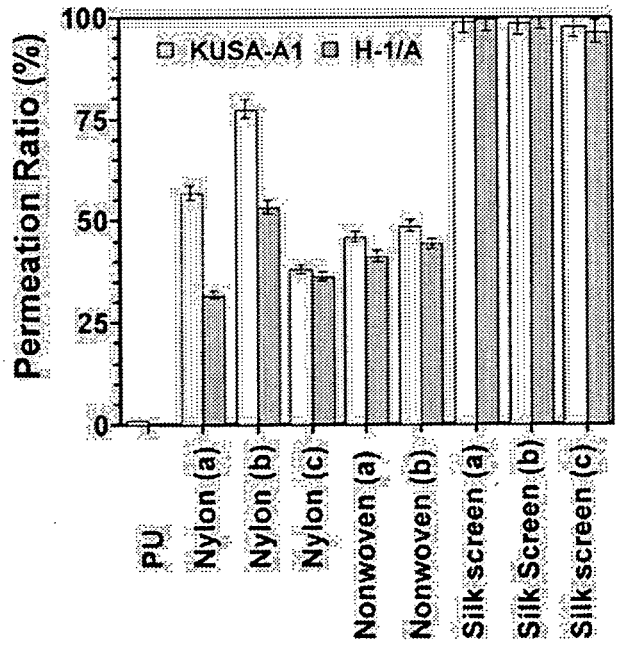

Figure 7. Permeation ratio of KUSA-A1 cells and H-1/A cells through PU, nylon-net filter [nylon (a)], nylon-net filter coated with fibronectin [nylon (b)] and collagen [nylon (c)], nonwoven fabrics made of acrylonitrile [nonwoven (a)], nylon and polyester [nonwoven (b)], and silk screens made of silk [silk screen (a), mesh size 150] and Tetron™ [silk screen (b), mesh size 150 and silk screen (c), mesh size 250] after permeation of mixed-cell solution at the cell density of 50,000 cells/mL and 25°C. Data are expressed as the means ± standard deviation of four independent measurements.

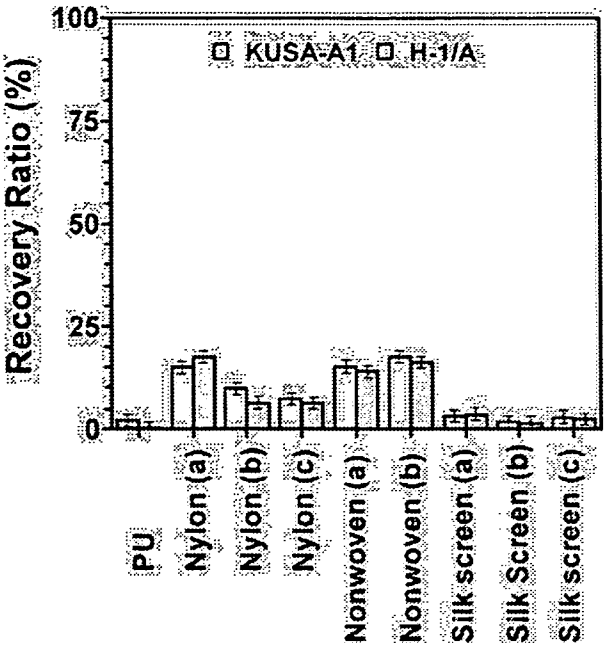

Figure 8. Recovery ratio of KUSA-A1 cells and H-1/A cells through PU, nylon-net filter [nylon (a)], nylon-net filter coated with fibronectin [nylon (b)] and collagen [nylon (c)], nonwoven fabrics made of acrylonitrile [nonwoven (a)], nylon and polyester [nonwoven (b)], and silk screens made of silk [silk screen (a), mesh size 150] and Tetron™ [silk screen (b), mesh size 150 and silk screen (c), mesh size 250] after permeation of mixed-cell solution at the cell density of 50,000 cells/mL and 25°C. Data are expressed as the means ± standard deviation of four independent measurements.

This is mainly due to the smaller cell size of the KUSA-A1 cells as detected in the forward and side light scattering intensities shown in [Figure 1(b)]. In addition, a high cell permeation ratio was also found with the use of silk screens made of silk or Tetron™. This was because silk screens have a larger pore size than the nylon-net filter and PU membranes (see Figure 2). A relatively good separation factor for permeation (α_p), defined as the relative permeation ratio of KUSA-A1 cells divided by that of H-1/A cells, was obtained when the mixed-cell solution was passed through the nylon-net filter (α_p = 1.8) or fibronectin-coated nylon-net filter (α_p = 1.5) membranes, whereas a separation was not obtained when the nonwoven fabrics or silk screens were used. Overall, the results suggest that the pore size of nylon-net filter was optimal for producing a sieving effect.

The effect of passing the HSA solution through the porous polymeric membranes after permeation of the cell mixture was also assessed. As shown in Figure 8, the recovery ratio of both KUSA-A1 and H-1/A cells was relatively low (< 20%) for all of the membranes. This is caused by the high adhesiveness of the mesenchymal cells and their high permeation ratio. Analysis of the recovery solution shows that there was no effective separation of KUSA-A1 and H-1/A cells. This is probably due to the fact that the KUSA-A1 and H-1/A cells are both mesenchymal cells and have similar characteristics (i.e., adhesiveness).

CONCLUSIONS

These results show that a separation of cells with similar characteristics, such as different types of mesenchymal cells (i.e., osteoblasts and preadipocytes) can be obtained in the permeate solution, but not in the recovery solution following membrane filtration. The main factor in this separation is the sieving effect of cells through the porous membranes. Therefore, prior to separation, flow cytometry should be carried out to confirm that the cells to be separated have different sizes. Separation factor, (α_p = 1.8) and a high permeation ratio was achieved when a mixed-cell solution was passed through a nylon-net filter with an 11-μm poor size, whereas an extremely low permeation ratio (< 5%) of both cell types was found with the use of surface-modified or unmodified PU foaming membranes with a 12-μm pore size. It was also found that the nylon-net filter had screen-like pore structure, whereas the PU membranes had a deformed open pore structure. This indicates that not only the pore size but also the pore morphology is important for membrane-based cell separation.

Even a small degree of enrichment, such as the separation factor of 1.8, is also considered effective in the transplantation of mesenchymal cells in clinical application, although clinical trials using the enriched-cell type of mesenchymal cells have not yet been performed. In conclusion, cell separation between mesenchymal progenitor cells through porous polymeric membranes was shown to be possible in this study. This technology will contribute to the future clinical application of cell transplantation into the damaged tissue of patients.

REFERENCES

1. Umezawa A, Maruyama T, Segawa K, Shadduck RK, Waheed A, Hata J. Multipotent marrow stromal cell is able to induce hematopoiesis *in vivo*. J Cell Physiol 1992;151:197–205.
2. Kohyama J, Abe H, Shimazaki T, Koizumi A, Nakashima K, Gojo S, Taga T, Okano H, Hata J, Umezawa A. Brain from bone: Efficient "meta-differentiation" of marrow stroma-derived mature osteoblasts to neurons with Noggin or a demethylating agent. Differentiation 2001;68:235–244.
3. Edwards M, Twin J, Wilkinson S. New technique to assess the axilla for breast cancer metastases using cell separation technology. Aust N Z J Surg 2002;72:655–659.
4. Vij R, Brown R, Shenoy S, Haug JS, Kaesberg D, Adkins D, Goodnough LT, Khoury H, DiPersio J. Allogeneic peripheral blood stem cell transplantation following $CD34^+$ enrichment by density gradient separation. Bone Marrow Transplant 2000; 25:1223–1228.
5. Sanada Y. Transplantation of hematopoietic cells: General theory. In: Harada M, Katoh S, Sanada Y, editors. New trends in hematopoietic stem cell transplantation. Tokyo: Nanoudo: 1998. p 1–7.
6. Gryn J, Shadduck RK, Lister J, Zeigler ZR, Raymond JM. Factors affecting purification of $CD34^+$ peripheral blood stem cells using the Baxter Isolex 300i. J Hematother Stem Cell Res 2002;11:719–730.
7. Carreras E, Saiz A, Marin P, Martinez C, Rovira M, Villamor N, Aymerich M, Lozano M, Fernandez-Aviles F, Urbano-Izpizua A, Montserrat E, Graus F. $CD34^+$ selected autologous

peripheral blood stem cell transplantation for multiple sclerosis: report of toxicity and treatment results at one year of follow-up in 15 patients. Haematologica 2003;88:306–314.
8. Domingo JC, Mercadal M, Petriz J, De Madariaga MA. Preparation of PEG-grafted immunomagnetoliposomes entrapping citrate stabilized magnetite particles and their application in $CD34^+$ cell sorting. J Microencapsul 2001;18:41–54.
9. Comella K, Nakamura M, Melnik K, Chosy J, Zborowski M, Cooper MA, Fehniger TA, Caligiuri MA, Chalmers JJ. Effects of antibody concentration on the separation of human natural killer cells in a commercial immunomagnetic separation system. Cytometry 2001;45:285–293.
10. Kataoka K, Sakurai Y, Hanai T, Maruyama A, Tsuruta T. Immunoaffinity chromatography of lymphocyte subpopulations using *tert*-amine derived matrices with adsorbed antibodies. Biomaterials 1988;9:218–224.
11. Ohba H, Bakalova R, Moriwaki S, Nakamura O. Fractionation of normal and leukemic T-cells by lectin-affinity column chromatography. Cancer Lett 2002;184:207–214.
12. Komai H, Naito Y, Fujiwara K, Takagaki Y, Noguchi Y, Nishimura Y. The protective effect of a leucocyte removal filter on the lung in open-heart surgery for ventricular septal defect. Perfusion 1998;13:27–34.
13. Muller-Steinhardt M, Hennig H, Kirchner H, Schlenke P. Prestorage WBC filtration of RBC units with soft-shell filters: filtration performance and impact on RBCs during storage for 42 days. Transfusion 2002;42:153–158.
14. Higuchi A, Yamamiya S, Yoon BO, Sakurai N, Hara M. Peripheral blood cell separation through surface-modified polyurethane membranes. J Biomed Mater Res 2004;68:34–42.
15. Kiyohara S, Sasaki M, Saito K, Sugita K, Sugo T. Radiation-induced grafting of phenylalanine-containing monomer onto a porous membrane. Reactive Functional Polym 1996;31:103–110.
16. Kim M, Kiyohara S, Konishi S, Tsuneda S, Saito K, Sugo T. Ring-opening reaction of poly-GMA chain grafted onto a porous membrane. J Membrane Sci 1996;117:33–38.
17. Higuchi A, Takanashi Y, Tsuzuki N, Asakura T, Cho CS, Akaike T, Hara M. Production of interferon-β by fibroblast cells on membranes prepared with RGD-containing peptides. J Biomed Mater Res 2003;65:369–378.
18. Higuchi A, Takanashi Y, Ohno T, Asakura T, Cho CS, Akaike T, Hara M. Production of interferon-β by fibroblast cells on the membranes prepared by extracellular matrix proteins. Cytotechnology 2002;39:131–137.
19. Higuchi A, Tamiya S, Tsubomura T, Katoh A, Cho CS, Akaike T, Hara M. Growth of L929 cells on polymeric films prepared by Langmuir-Blodgett and casting methods. J Biomater Sci Polym Ed 2000;11:149–168.
20. Higuchi A, Shirano K, Harashima M, Yoon BO, Hara M, Hattori M, Imamura K. Chemically modified polysulfone hollow fibers with vinylpyrrolidone having improved blood compatibility. Biomaterials 2002;23:2659–2666.
21. Keeney M, Chin-Yee I, Weir K, Popma J, Nayar R, Sutherlamd DR. Single platform flow cytometric absolute $CD34^+$ cell counts based on the ISAHE guidelines. Cytometry 1998; 34:61–70.

Available online at www.sciencedirect.com
SCIENCE DIRECT
ELSEVIER
Cancer Letters 221 (2005) 21–28
CANCER Letters
www.elsevier.com/locate/canlet

Effects of 3-methylcholanthrene on the transcriptional activity and mRNA accumulation of the oncogene *hWAPL*

Masahiko Kuroda[a,b,c,*], Kosuke Oikawa[a,b,c], Keiichi Yoshida[a,c], Aya Takeuchi[d], Masaru Takeuchi[d], Masahiko Usui[d], Akihiro Umezawa[c,e], Kiyoshi Mukai[a]

[a]*Department of Pathology, Tokyo Medical University, 6-1-1 Shinjuku, Shinjuku-ku, Tokyo 160-8402, Japan*
[b]*CREST Research Project, Japan Science and Technology Corporation, 4-1-6 Kawaguchi, Saitama 332-0012, Japan*
[c]*Shinanomachi Research Park, Keio University, 35 Shinanomachi, Shinjuku-ku, Tokyo 160-8582, Japan*
[d]*Department of Ophthalmology, Tokyo Medical University, 6-7-1 Nishi-shinjuku, Shinjuku-ku, Tokyo 160-0023, Japan*
[e]*National Research Institute for Child Health and Development, 3-35-31 Taishido, Setagaya-ku, Tokyo 154-8567, Japan*

Received 28 April 2004; received in revised form 26 July 2004; accepted 5 August 2004

Abstract

hWAPL is a human oncogene associated with uterine cervical cancer. Here, we demonstrate that *hWAPL* transcription is induced by 3-methylcholanthrene (3-MC) in the cervical carcinoma-derived cell line SiHa. *hWAPL* transcription was analyzed with evaluation of the mRNA and heterogeneous nuclear RNA (hnRNA) levels by quantitative real time PCR analysis. Flow cytometric analysis suggested that the alteration of *hWAPL* mRNA levels is independent of cell cycle profile. We also found that DMSO and some components of FBS affect *hWAPL* transcription. Interestingly, when the aryl hydrocarbon receptor (AhR) function was inhibited by α-naphthoflavone (ANF), the induction of *hWAPL* transcription by 3-MC was greater than that in AhR-functioning normal cells. These observations suggest that there are complex mechanisms regulating the transcription of *hWAPL*. Furthermore, mRNA level of a mouse homolog of *hWAPL* in mouse uterus was induced by 3-MC injection into the abdominal cavity. Thus, some effects from 3-MC exposure on uterus may be mediated by the unscheduled overexpression of *hWAPL*.

Keywords: 3-Methylcholanthrene (3-MC); hWAPL; Uterine cervical cancer; Aryl hydrocarbon receptor (AhR); α-naphthoflavone (ANF)

1. Introduction

Previously, we have isolated and characterized a novel human gene termed *hWAPL* [1]. Our initial observations suggested that *hWAPL* expression is associated with uterine cervical cancer, although the mechanism was not clear. *hWAPL* is the human homolog of the *wings apart-like* (*wapl*) gene in

* Corresponding author. Address: Department of Pathology, Tokyo Medical University, 6-1-1 Shinjuku, Shinjuku-ku, Tokyo 160-8402, Japan. Tel.: +81 3 3351 6141x425; fax: +81 3 3352 6335.
E-mail address: kuroda@tokyo-med.ac.jp (M. Kuroda).

0304-3835/$ - see front matter © 2004 Elsevier Ireland Ltd. All rights reserved.
doi:10.1016/j.canlet.2004.08.006

Drosophila melanogaster. The protein encoded by *wapl* controls heterochromatin organization and was identified as a modifier of both PEV and chromosome inheritance [2,3]. Thus, hWAPL is also expected to be involved in heterochromatin maintenance and epigenetic control.

Polycyclic aromatic hydrocarbons (PAHs) are carcinogenic and immunotoxic chemicals widely distributed in the environment [4]. 3-Methylcholanthrene (3-MC) is one of the most toxic and the best-studied compounds in the PAHs. Most of the toxic effects of PAHs are mediated by the aryl hydrocarbon receptor (AhR) [5]. When PAHs bind to the AhR, the ligated AhR translocates from the cytoplasm to the nucleus where it switches its partner molecule from heat shock protein 90 kD (Hsp90) to the aryl hydrocarbon receptor nuclear translocator (Arnt) [6]. The resulting AhR/Arnt heterodimer binds a specific DNA sequence, designated xenobiotic responsive element (XRE), in the promoter region of target genes to enhance their expression [6]. On the other hand, several studies have suggested the existence of AhR independent pathways for PAH toxicity [7,8]. In all cases, many of the putative target genes responsible for the toxicity symptoms have yet to be identified.

In the present study, we demonstrate that *hWAPL* is a target gene of 3-methylcholanthrene. The results suggest that carcinogenesis by 3-MC may involve alterations of *hWAPL* gene expression.

2. Materials and methods

2.1. Chemicals

3-Methylcholanthrene (Sigma-Aldrich Japan, Tokyo, Japan) was prepared in dimethylsulfoxide (DMSO) for cultured cells and in olive oil for treatment of mice. Aphidicolin (Wako Pure Chemical Industries, Ltd, Osaka, Japan), Nocodazole (Sigma Chemical Co., St Louis, MO) and α-naphthoflavone (Sigma) were prepared in DMSO.

2.2. Cell cultures

The human uterine cervical carcinoma-derived cell lines, SiHa, CaSki and HeLa cells, were obtained from American Type Culture Collection (ATCC), and grown in DMEM (Sigma) supplemented with 10% fetal bovine serum (FBS) (Trace Scientific Ltd, Melbourne, Australia) at 37 °C in a 5% CO_2 environment. Where indicated, SiHa cells were grown in DMEM supplemented with 10% charcoal/dextran treated FBS (CTF) (Biosource, Rockville, MD) or 0.4% (w/v) bovine serum albumin (BSA) (Trace) instead of FBS.

2.3. Immunoblot analysis

Protein samples were prepared as previously described [9]. Immunoblot analysis was performed as previously described [1].

2.4. Flow cytometric analysis

To determine cell cycle profiles, cells at different time points were harvested, washed, and fixed with a solution containing 70% ethanol and 30% PBS. After incubation overnight at 4 °C, cells were suspended in staining buffer (propidium iodide, 50 μg/ml; RNaseA, 0.1%; glucose, 1 mg/ml in PBS). Then, after incubation for 30 min at room temperature, the cells were analyzed with a FACS Vantage flow cytometer using the Cell Quest acquisition and analysis program (BD Biosciences, San Jose, CA).

2.5. Animals and treatment

C57/BL6 female mice (6 weeks old) were purchased from Oriental Yeast Co., Ltd (Tokyo, Japan). The mice received a single intraperitoneal injection of 1 ml of olive oil containing 3-MC at a dose of 80 mg/kg of body mass. The control mice were injected with olive oil alone. Uterus samples were harvested 24 and 48 h after injection and subjected to real time PCR analysis.

2.6. RNA isolation and quantitative real time PCR

First strand cDNA synthesis was performed as described [10] using M-MLV Reverse transcriptase (Invitrogen Japan, Tokyo, Japan) with Oligo $(dT)_{17}$ (for Figs. 1–3 and 6) or Random Primers (Invitrogen) (for Figs. 4 and 5).

Real time PCR analysis for *hWAPL* and human β-*actin* mRNAs was performed as described [1]